EARLY AGE CRACKS IN CONCRETE WALLS

D. S. Hettiarachchi

(138735A)

Degree of Master of Science

Department of Civil Engineering

University of Moratuwa
Sri Lanka

November 2017

Declaration

I declare that this is my own work and this thesis does not incorporate without acknowledgement any material previously submitted for a Degree or Diploma in any other University or institute of higher learning and to the best of my knowledge and belief it does not contain any material previously published or written by another person except where the acknowledgement is made in the text.

Also, I hereby grant to University of Moratuwa the non-exclusive right to reproduce and distribute my thesis, in whole or in part in print, electronic or other medium. I retain the right to use this content in whole or part in future works.

Signature Date

The above candidate has carried out research for the Masters Dissertation under my supervision

Signature of the Supervisor Date

Abstract

Construction of a concrete structure requires a large volume of concrete. Due to the small surface area-to-volume ratio, concrete structures are often subjected to high potential of thermal cracking, caused by the heat generation from cement hydration. To reduce the thermal cracking and ensure structural integrity, a good understanding about the crack patterns in concrete elements is required. These kinds of cracks mostly occur during the early age state of concrete. Since Sri Lanka is very near to the equator, the probability of early age crack occurring is even higher.

The purpose of this research is to explore the potential early age crack patterns in vertical concrete walls. Main reason for the early age cracking in vertical walls are shrinkage and thermal contraction. This research focuses on the understanding of early age thermal cracking in concrete and developing a simple method to model this phenomenal computationally. Series of boundary conditions were modelled to obtain stress distributions using walls 3m high and 4m & 8m long. Boundary conditions were imposed according to guidelines in BS8007 and wall thickness maintained as 300mm during the analysis. All the analysis was carried out using FEM commercial software Sap 2000 (V19.1). Two approaches were followed initially to identify the best method to represent the restraint conditions as per BS8007. End restraints reduced by using roller supports up to a 2.4m distance from the free edge of the wall with gradually increasing applied horizontal forces proved to be the better technique than that of using reduced E-values.

The case studies yielded the following general findings that agree with the literature and field observations;

(i) 4m walls can have possible vertical and horizontal cracks.
(ii) 8m walls can have possible cracks approximately 2.4m away from the free edges with an inclination of approximately 45º-60º.
(iii) 8m walls get the highest stress close to 2.4m from the free edges whereas the 4m walls get the highest stress at the centre.
(iv) In 8m walls higher stresses are distributed over a central length whereas in 4m walls the higher stress is concentrated at the centre.
(v) 4m wall with top movement can cause possible inclined cracks.
(vi) 8m wall with top movement can lead to two possible dominant cracks and two minor cracks.

This validation was done qualitatively using the literature and on-site observations.

Key Words: Early age cracking, concrete, walls, thermal cracking

Acknowledgement

I would first like to express my greatest gratitude to my supervisor, Prof. Priyan Dias of the Department of Civil Engineering at University of Moratuwa. The door to Prof. Dias's office was always open whenever I ran into a trouble spot or had a question about my research or writing. He consistently allowed this paper to be my own work, but steered me in the right the direction whenever he thought I needed it.

I would also like to thank the Eng. Shiromal Fernando, who has been my superior and my mentor from the first day of my career. Without his guidance and encouragement, completing this work would have been impossible.

Finally, I must express my very profound gratitude to my parents and to my wife for providing me with unfailing support and continuous encouragement throughout my years of study and through the process of researching and writing this thesis. This accomplishment would not have been possible without them. Thank you.

Table of Contents

List of Figures

List of Tables

List of Abbreviations

ASTM	American Society for Testing and Materials
RH	Relative Humidity

1 Introduction

Sri Lanka's high-rise building industry mostly incorporates a common method of a beam –slab load carrying system up to a transfer floor (to compensate the different grid systems in parking and apartment levels) and the upper floors supported by a shear wall arrangement there onwards. These shear walls are part of the vertical load transfer system as well as the lateral load transfer system thus making them crucial elements in the structure. It is therefore of utmost importance to ensure these walls are subjected to minimum amounts of cracks at the initial stages.

Cracks may develop in concrete structures due to variety of reasons. Other than the structural and serviceability issues, cracks could affect the appearance of the structure. Concrete is a quasi-brittle material with a low capacity for deformation under tensile stresses. Visible cracking occurs when the tensile stresses exceed the tensile strength of the material. The exceeding of tensile strength could happen due to mechanical loadings, reactions on surface and environmental conditions.

Major purpose of this study is about early age cracks in concrete walls (vertical shear walls). Most of the cracks occur during the hardening period of mass concrete. These hardening periods are divided into two major process, they are "before hardening period" and "after hardening period". In this research we will mainly discuss temperature variation of concrete walls in early age (initial state) and crack propagation in vertical walls. Figure 01 shows concrete wall crack of an ongoing local project located in Colombo and an enlarged view of the crack.

1.1 Aim & Scope

Early age cracking is a severe problem in concrete structures and components. It is important to understand, that all cracks may have different causes and different effects on long term performance of structures. Early age cracks occur due to volume changes mainly due to shrinkage and temperature variations during the immature stage of concrete. This research will primarily focus on the early age cracking due to temperature variations in concrete walls. In this research, a numerical model will be implemented to compare results with past observations and thus to understand mechanisms and suggest improvements. The scope of this research is to provide some ready solutions towards making sure these cracks are minimized as much as possible and more importantly limited in propagation. For this purpose;

- A numerical analysis will be carried out.
- Past observations will be compared with the numerical model results.
- Early age crack propagation patterns will be identified in concrete.

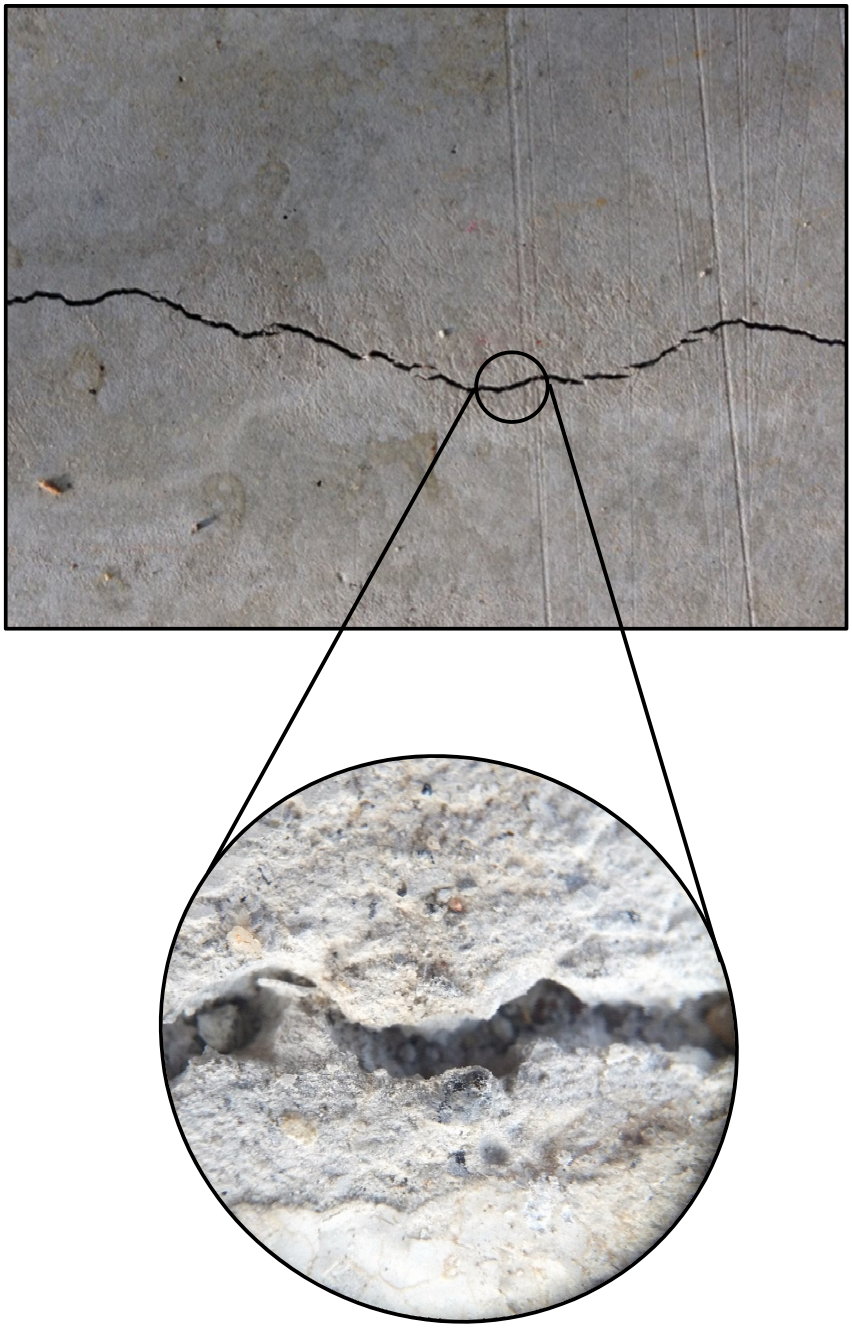

Figure 01: Observed early age cracks in local project Colombo

1.2 Methodology

Brief summary of this research and how the work is carried out, is presented in the below flow diagram.

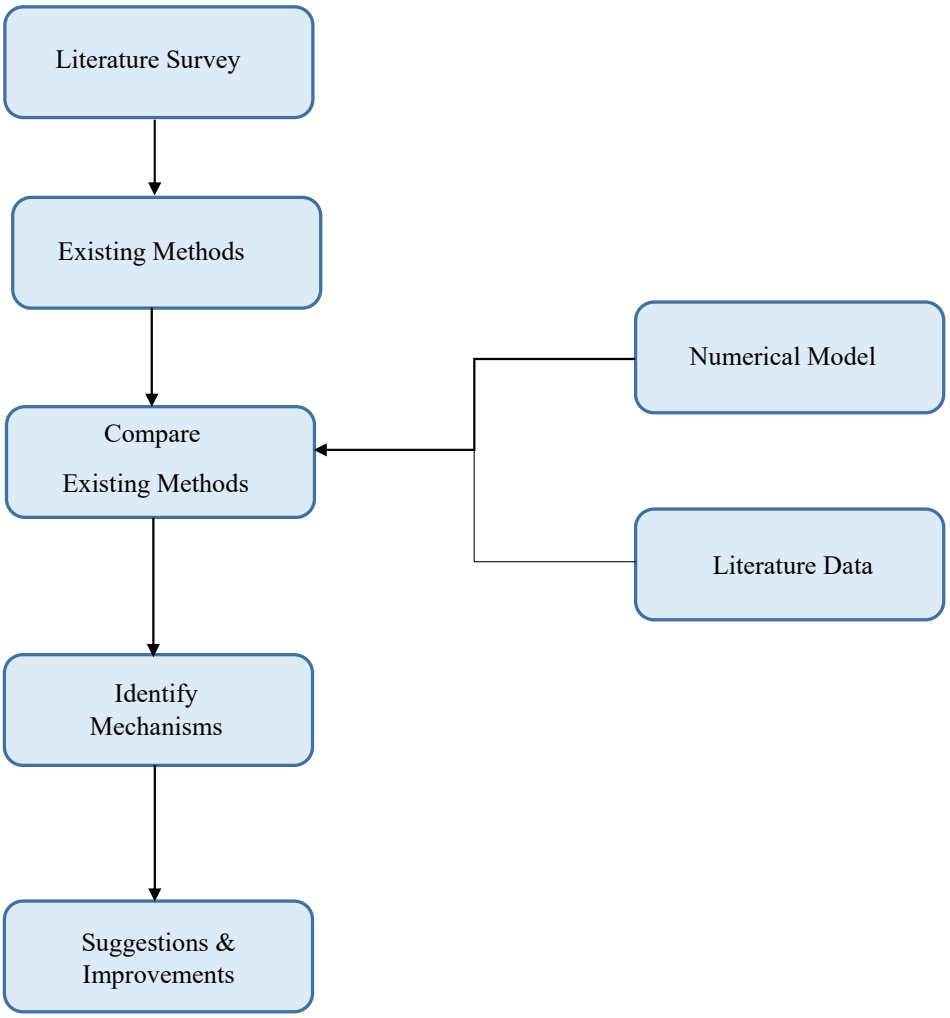

Figure 02: Flow diagram (methodology)

2 Review of Literature and Practice

2.1 Literature Review

This section presents a survey of literature. This is related to studies on early age cracking in concrete walls and comparison with past test data. Time of appearance of cracks before concrete hardening is from 10 minutes to 6 hours. These cracks appear primarily due to settlement, construction movements and excessive evaporation of water [Klemczak et al, 2011]. When the tensile stress exceeds the tensile strength of concrete cracks will occur in any situation. The concrete tensile strain limit is around 0.01-0.012 % [Leonhardt F.,1988]

Table 01 provides common types of cracks in concrete structures and stages at which they can occur.

Table 01: Types of cracks and their stages. [Klemczak et al, 2011]

<table>
<tr><th colspan="6">Types of Cracks</th></tr>
<tr><th colspan="2">Cracks occuring before hardening</th><th colspan="4">Cracks occuring after hardening</th></tr>
<tr><td colspan="2">Fresh Concrete</td><td colspan="2">Young Concrete(Early age,Immature Concrete)</td><td colspan="2">Mature Concrete</td></tr>
<tr><td rowspan="2">Construction Movement</td><td>Formwork Movement</td><td rowspan="6">Volume Changes</td><td rowspan="4">Autogenous and Drying Shrinkage</td><td rowspan="2">Structural Cracks</td><td>Design Load/Accidental Overload</td></tr>
<tr><td>Sub-Grade Movement</td><td>Fatigue</td></tr>
<tr><td rowspan="3">Plastic</td><td>Plastic Shrinkage</td><td rowspan="3">Volume Changes</td><td>Drying Shrinkage</td></tr>
<tr><td>Plastic Settlement</td><td>External Seasonal Temperature Variation</td></tr>
<tr><td>Autogenous Shrinkage</td><td rowspan="4">Temperature Variations Due to Hydration Process</td><td rowspan="4">Physio-Chemical</td><td>Corrosion of R/F</td></tr>
<tr><td rowspan="2">Frost Damage</td><td>Premature Freezing</td><td>Freeze-Thaw Cycling</td></tr>
<tr><td>Scaling Crazing</td><td>Alkali Aggregate Reactions</td></tr>
<tr><td></td><td></td><td>Cement Carbonation</td></tr>
</table>

2.1.1 Early Age Concrete

Physical and mechanical properties of concrete undergo continuous changes from the moment of mixing of the concrete constituents up to the moment of achieving their final values in the mature concrete. Development of these properties is connected with the progressing process of cement hydration and its advancement depends directly on the degree of hydration [Schutter & Tarewe, 1996] (Figure 03).

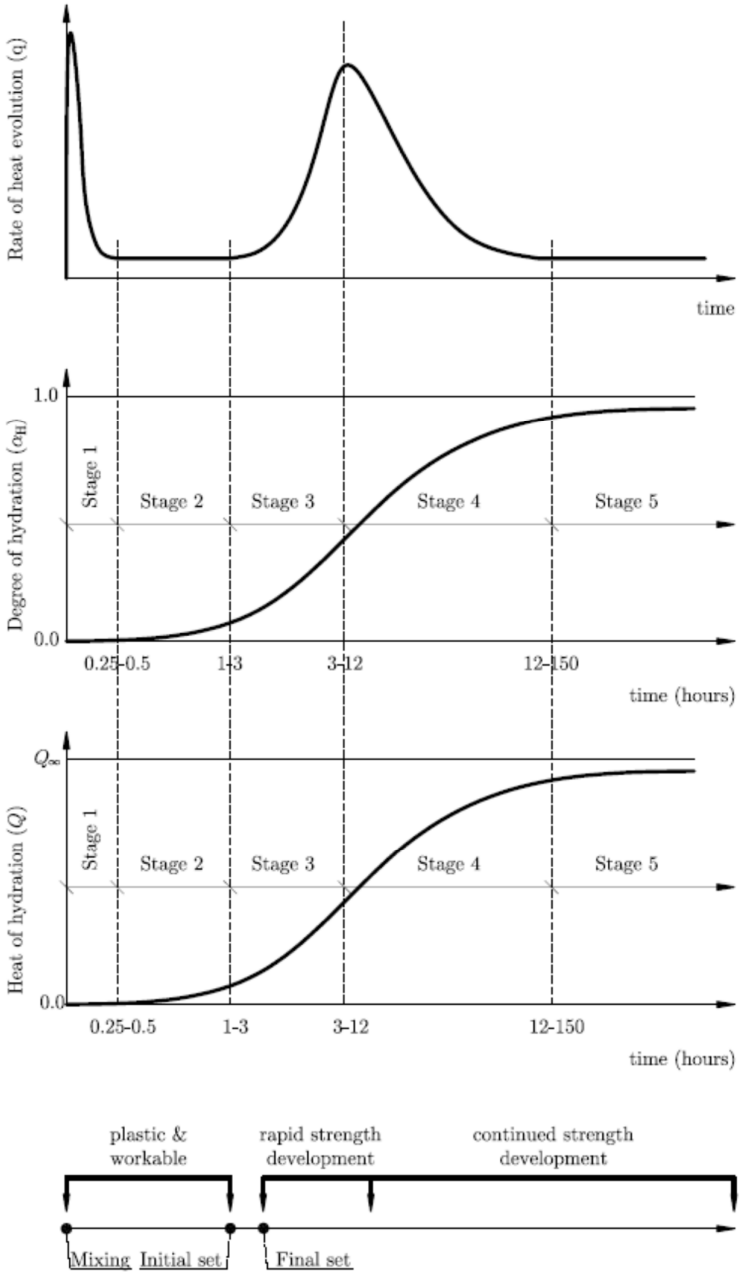

Figure 03: Concrete behaviour during progressing hydration of cement [Schindler, 2002]

Three main characteristic phases in concrete life can be distinguished: fresh concrete, early-age concrete (transient phase) and mature concrete [Knoppik, 2015]. Fresh concrete is a multi-component material, composed of aggregate, cement and water, characterised by properties of a plastic material and liquid. This phase of concrete is workable and allows for transportation and casting until the setting process begins. According to the development of hydration heat, in the first stage after mixing (stage 1) a rapid increase of heat production is observed, which is connected with wetting of cement grains. Then, the rate of heat production decelerates almost completely (stage 2); this phase is called a dormant period [Neville, 2012]. Fresh concrete generally does not have strength. Due to capillary pressure and friction between the concrete mix constituents it is possible to determine the instantaneous strength of fresh concrete but it is an apparent strength.

Setting of concrete initiates a few (1 to 3) hours after mixing. When setting begins, the rate of hydration heat development increases (stage 3), but with a slower rate than in the stage 1; C–S–H gel is produced in that phase. As soon as the setting of the concrete mix is terminated, concrete can be regarded as a solid material, characterised by elastic, plastic and also strong viscous properties. This phase is called early-age concrete. Progressing cement hydration leads to strength development in concrete. An increased rate of strength development is observed in the very early ages of concrete hardening connected with an increase in the rate of hydration heat development (stage 3). Then, the hydration process decelerates again (stage 4) and so does the rate of strength development. In some types of cements second peak in the rate of hydration heat development might be observed [Neville, 2012].

Theoretically, the strength gain proceeds until the hydration of cement is completed (stage 5). Then the concrete strength reaches its final, steady value. Practically, the hydration process is never completed and strength gain continues in mature concrete. However, for practical reasons, it is assumed that hardening of concrete terminates after 28 days, the concrete at that moment is considered as mature and its strength as final. Nevertheless, it was observed that in concrete mixes made of blended cements hydration rate is slower and significant gain in material properties occurs way beyond 28th day [Knoppik, 2015].

Due to the exothermic character of cement hydration temperature development is observed in concrete elements. The process of concrete hardening is also accompanied with moisture migration which leads to reduction of concrete volume and consequent shrinkage of a concrete element. Water is transported within and out of the concrete element due to various phenomena.

2.1.2 Early Age Cracking

At the after hardening period concrete will be categorized into two phases, which is called immature concrete and mature concrete. During the immature concrete period early age cracks will occur.

The major reasons of cracking in early age concrete is the volume changes due to the temperature and moisture variations during hardening process. The variations of the concrete temperature during curing are the result of heat release process nature of the chemical reaction between cement and water. When cement is mixed with water, heat is released due to chemical reaction and this is called the heat of hydration. This heat dissipates relatively quickly in thin concrete sections and causes no problems. In thicker sections, due to the poor thermal conductivity of concrete, high temperature gradients may occur between the internal surface and the surface of structural elements.

Concrete curing is also accompanied with a moisture exchange with the environment in conditions of variable temperatures. The loss of water through evaporation at the surface of element results in shrinkage, which is classified as an external drying shrinkage. There is also internal drying resulting from the reduction in material volume as water is consumed by hydration, which is classified as autogenous shrinkage [Klemczak et al, 2011]. Summary of the study area has been provided in below flow diagram (Figure 04)

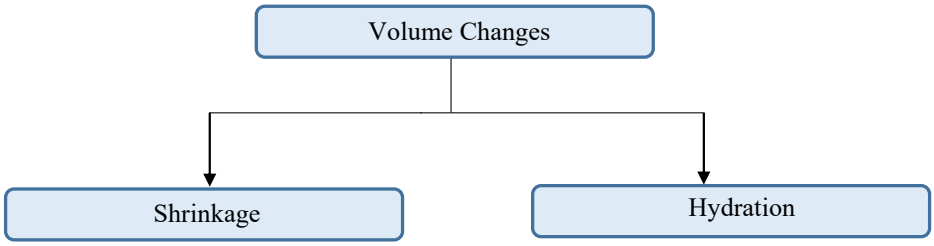

- External drying shrinkage.
- Autogenous shrinkage.

Figure 04: Study areas

2.1.3 Shrinkage

Shrinkage is the action of reduction of size of concrete due to water getting removed from the concrete or consumed within the element. When a restraint to this is provided, tensile stresses tend to occur in the concrete. Figure 05 shows the moisture content development and shrinkage stress development for an externally-restrained concrete wall.

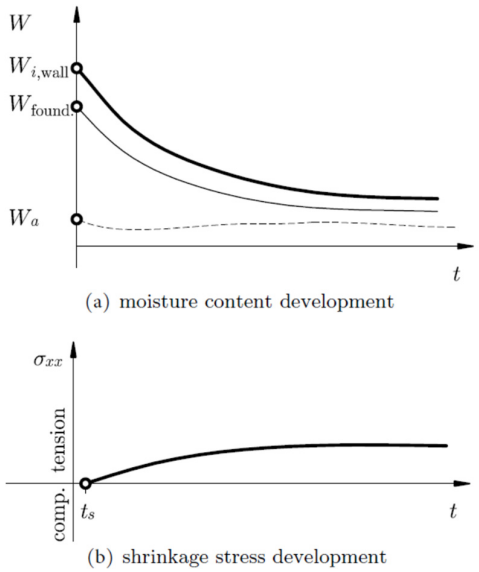

Figure 05: Moisture content, and shrinkage stress development with time in an externally-restrained concrete wall [Knoppik, 2015]

2.1.3.1 External Drying Shrinkage

The loss of water through evaporation at the surface of element results in shrinkage, which is classified as an external drying shrinkage. [Klemczak et al, 2011]

There are several factors affecting external drying shrinkage. These factors include the properties of the components, proportions of the components, mixing manner, amount of moisture while curing, dry environment, and member size. Concrete cured under environmental conditions will undergo some volumetric change. Drying shrinkage happens mostly because of the reduction of capillary water by evaporation. If water is higher in the fresh concrete, the greater the drying shrinkage effects. The shrinkage potential of a particular concrete is influenced by the amount of mixing, the elapsed time after the addition of water, temperature fluctuation, slump, placement, and curing. The constituents of concrete are also very important. Every aggregate and cement type have distinctive characteristics, each contributing to concrete shrinkage. The amounts of water and admixtures used during mixing also have direct and indirect effects on drying shrinkage of concrete.

2.1.3.2 Autogenous Shrinkage

Autogenous shrinkage is an important phenomenon in immature concrete at low water/cement ratios. All the water is rapidly drawn into the hydration process and the demand for more water creates very fine capillaries. The surface tension within the capillaries causes autogenous shrinkage (sometimes called self-desiccation) which can lead to cracking. This can be largely avoided by keeping the surface of the concrete continuously wet. Conventional curing by sealing the surface to prevent evaporation is not enough and water curing is essential. With wet curing, water is drawn into the capillaries and the shrinkage does not occur. Note that autogenous shrinkage is separate from and additional to external drying shrinkage, which will start when water curing ceases.

Figure 06: Chemical shrinkage cracks in concrete. [http://www.concrete.org.uk]

2.1.4 Temperature Variations Due to Hydration

The variation of the concrete temperature during curing are the result of exothermic nature of the chemical reaction between cement and water, when cement is mixed with water, heat is liberated and this heat is called the heat of hydration.

The factors affecting the heat of hydration are cement type, chemical composition, section dimensions, w/c ratio and admixtures. During the concrete hardening process two main phases can be distinguished in a concrete element behaviour according to the temperature change in time (Figure 07a): a phase of the concrete temperature increase (self-heating) and a phase of cooling of the element down to the temperature of the ambient air. The restrained wall extends in the first phase, opposed by the base, which results in formation of compressive stresses (Figure 07b, $t < t2$).

As soon as the maximum temperature is reached, the wall starts to cool down, restrained by the base. This leads to development of tensile stresses in the wall (Fig. 07b, t > t2). Development of stresses begins a few hours after casting of concrete, at the setting time, ts, when concrete starts to gain stiffness. The graphs in Figure 07 present generalised illustration of the discussed phenomena. The value of the temperature is different in each point of the wall so the values of the generated stresses vary within the wall due to different thermal and shrinkage strains as well as due to different degree of the restraint. Nevertheless, their character presented in Figure 07 is valid in most areas of the wall. Total tensile stresses in cooling phase concentrate near the joint and reach a significant height of the wall. These stresses may lead to cracking of the element. [Knoppik, 2015]

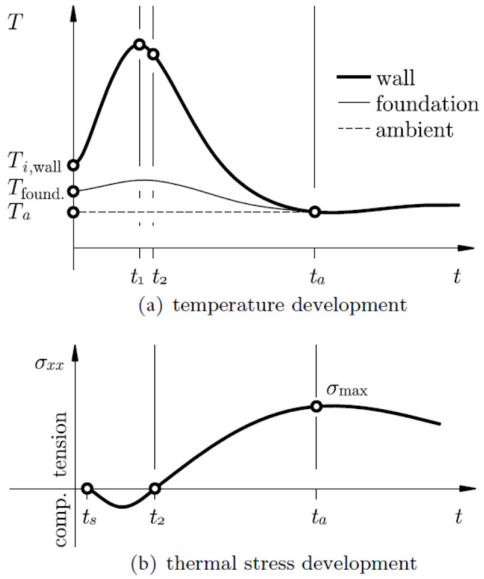

Figure 07: Temperature and thermal stress development in time in an externally-restrained concrete wall [Knoppik, 2015]

When concrete hardens, it gains considerable compressive strength but little tensile strength. Tensile strength of concrete is about one-tenth of its compressive strength. Also, concrete is a brittle material — when stretched, it cracks. When thermal stresses exceed the tensile strength of the concrete, cracking occurs.

A typical pattern of cracking due to the edge restraint of a wall is shown in Figure 08a, assuming that the base is rigid. Without a restraint the section would contract along the line of the base, and so with the restraint a horizontal force develops along the construction joint. The occurring cracks are vertical in the central part of the wall and splay towards the ends of the element where a vertical tensile force is required to balance the tendency of the horizontal force to warp the wall. A horizontal crack may occur at the construction joint at the ends of the walls due to this warping restraint.

Figure 08b presents the cracking of the wall with end restraint. The external restraint might be a combination of base and side restraint (Figure 08c, Figure 08d) [Klemczak, et al, 2011]. Usually the first crack occurs at the construction joint as the strength of the bond between the new and mature concrete is less than the tensile strength of the element. Such a crack is therefore less likely to be fully developed. If the overall contraction of the wall can be satisfied by fully developed cracks at one or both construction joints then the intermediate cracks shown in Figure 08c and Figure 08d may not occur. This explains why the worst cracks are usually seen at construction joints or at changes of section where stresses concentrate.

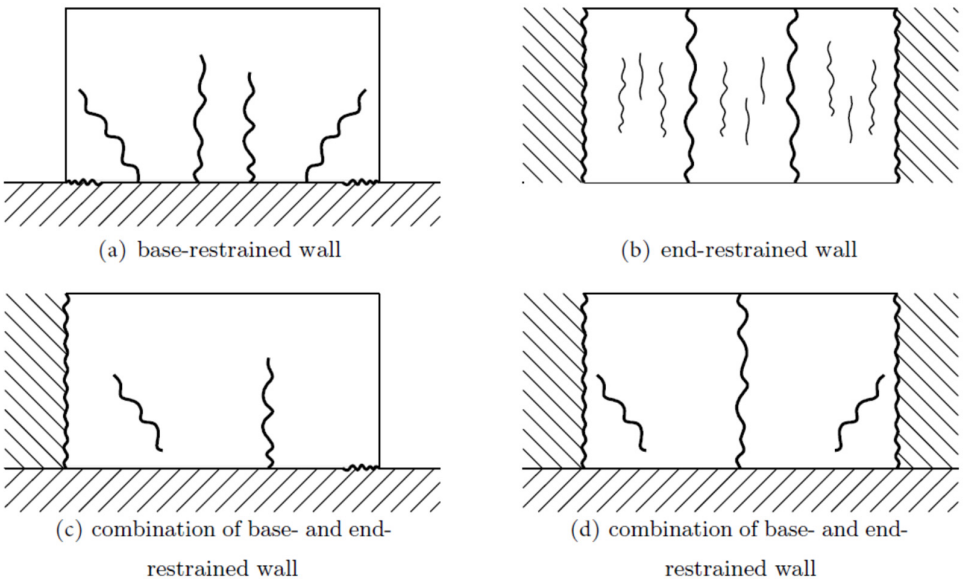

Figure 08: Typical cracking patterns in early-age reinforced concrete walls [Klemczak, et al, 2011]

The cracks run vertically, reach – depending on the wall length and height – up to ⅓, ½ or even ⅔ of the wall height. They are spaced at about 1.5-3.0 m, and maximum crack width, $w_{k,max}$ is 0.3-0.5 mm and appears at ⅓ of crack height. The cracks start close above the contact zone between the wall and foundation, they next widen, reaching the value of $w_{k,max}$ and reduce in width until they disappear.

Another property of these cracks is that their largest height appears in the middle of wall length, while this height is reduced towards its beginning and end (or towards the expansion joints), as shown approximately in Figure 09. [Flaga, Furtak, 2009]

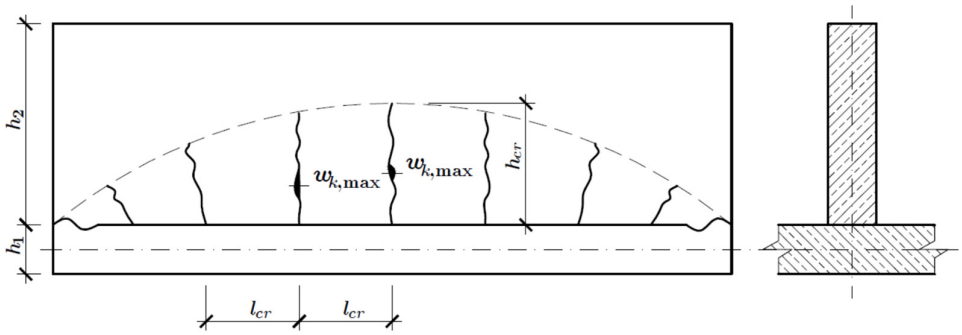

Figure 09: Cracking pattern in an externally-restrained reinforced concrete element [Flaga, Furtak, 2009]

2.1.5 Code Provisions

According to BS8007 crack patterns are varying according there restrains. Typical crack patterns mentioned in BS8007 is shown below.

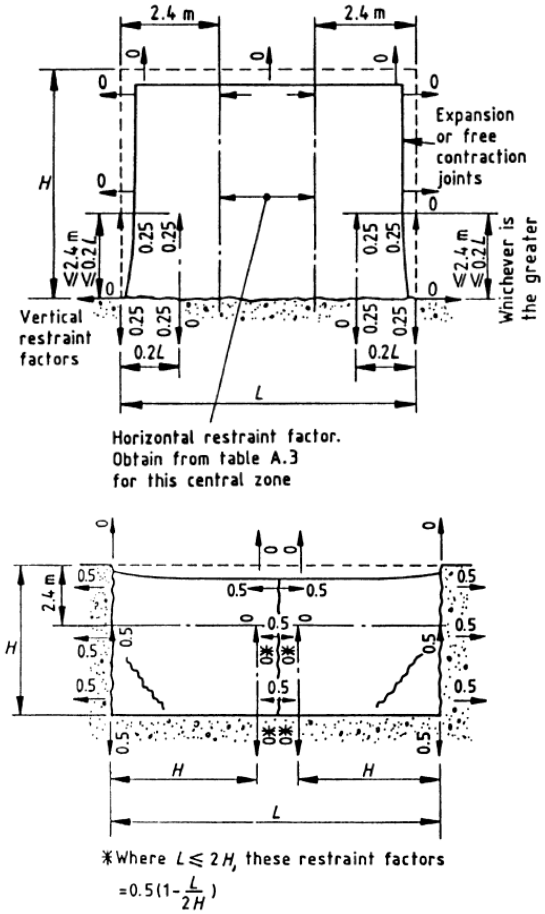

Figure 10: Various restraints [extracted from BS 8007: 1987]

2.2 Review of Practice

Currently, tall buildings are coming up at a considerable rate in Sri Lanka and most of them consist of a set of core walls and shear walls. These shear walls are cast either as freestanding (only with base restraint) or with slabs and beams (top and bottom restraint). Early age cracks are a common issue in these walls.

This section will focus on cracking occurred in a project in Colombo and the possible causes. The vertical load carrying system comprises of core walls, shear walls and columns. The shear wall thicknesses vary from 400mm-800mm. Concreting of slabs and walls/columns has been done simultaneously. Early age cracks have been observed in these walls vertically and diagonally. (Figure 11 and Figure 12)

Figure 11: Vertical crack observed [Project in Colombo]

Figure 12: Diagonal crack observed [Project in Colombo]

Further, it has been observed that vertical cracks are prominent in the core walls while the diagonal cracks are prominent in the stand-alone walls. Also, the walls at the edges were observed with two dominant diagonal cracks and two smaller diagonal cracks (Figure 13). It is suspected that the higher amount of shrinkage movement at the edges could cause the freshly cast floor above to move thus creating this crack pattern.

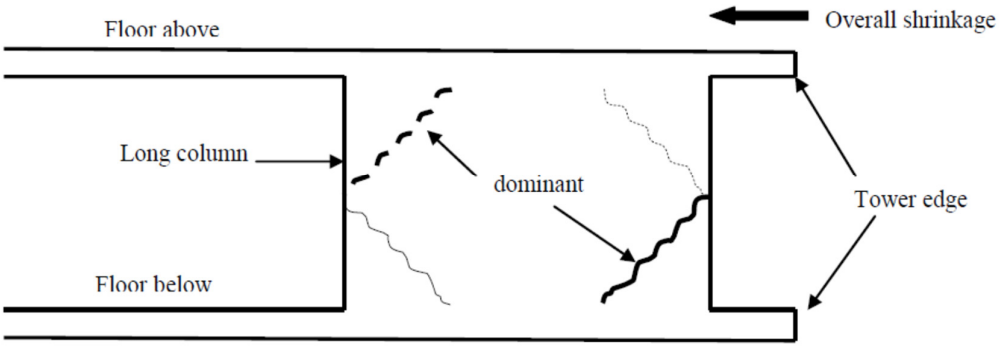

Figure 13: Schematic diagram of diagonal cracking in edge walls

3 Approach to Modelling

3.1 Initial Modelling

SAP 2000 FEM software was used for modelling and the initial modelling was done for a 300mm thick wall of 8m long and 3m high with base restraint. Shell elements were used and a coarse mesh of 0.400m x 0.375m was used for initial modelling.

As the temperature drop in the walls are causing the early age cracking, a temperature drop of -30ºC was used for the modelling. Initial model was done with a set of pinned support at the bottom at each node to represent the base restraint. Principal stress plot is shown in the Figure 14.

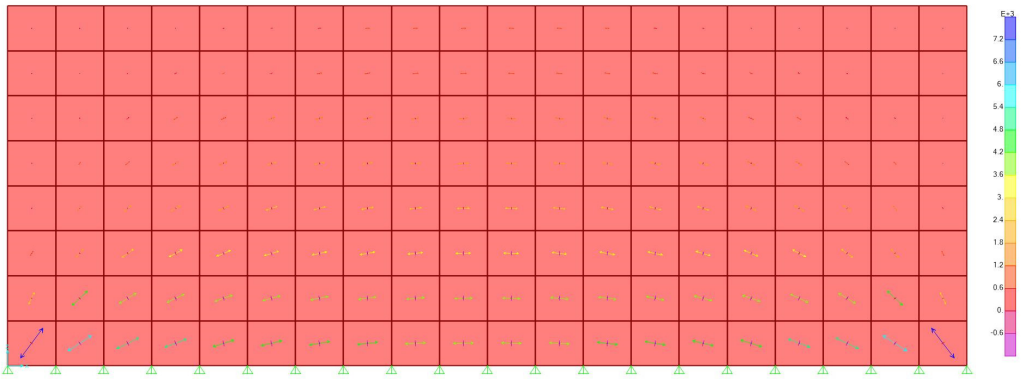

Figure 14: 8m wall with base restraint – bottom fully pinned

The results showed the maximum tensile stress at the edge of the wall. However, the actual crack pattern and thus the stress pattern should be as per Figure 09. Maximum stress shall be at the centre reducing up to the edge. Due to the curling effect at the edges, the principal stresses should be vertical to create the horizontal separation. Further, as per the external restraint factors given in BS8007:1987, the horizontal restraint shall be zero at the wall edge gradually increasing to 0.5 over a length of 2.4m. To represent this phenomenon, we looked into two modelling techniques.

1. Technique 1 – Reduced E Value in the Bottom Cells
2. Technique 2 – End Rollers with Forces

3.1.1 Technique 1 – Reduced E Value in the Bottom Cells

Since we are working with the early age effects, Young's modulus (hereinafter referred as E Value) in general is used as half the value of matured concrete. Young's modulus is taken as 30kN/mm^2 for mature concrete and 15kN/mm^2 for immature concrete.

Considering the restraint is changing from zero to 0.5 over a length of 2.4m, E values were gradually reduced from a distance of 2.4m from either side to the edge as shown in Figure 15. The empirical length of 2.4m was taken from BS8007:1987.

$\frac{E}{2}X\frac{1}{120}$	$\frac{E}{2}X\frac{1}{12}$	$\frac{E}{2}X\frac{2}{12}$	$\frac{E}{2}X\frac{3}{12}$	$\frac{E}{2}X\frac{4}{12}$	$\frac{E}{2}X\frac{5}{12}$	$\frac{E}{2}X\frac{6}{12}$	$\frac{E}{2}X\frac{7}{12}$	$\frac{E}{2}X\frac{8}{12}$	$\frac{E}{2}X\frac{9}{12}$	$\frac{E}{2}X\frac{10}{12}$	$\frac{E}{2}X\frac{11}{12}$
0.125 kN/m^2	1.25 kN/m^2	2.50 kN/m^2	3.75 kN/m^2	5.00 kN/m^2	6.75 kN/m^2	7.50 kN/m^2	8.75 kN/m^2	10.00 kN/m^2	11.25 kN/m^2	12.50 kN/m^2	13.75 kN/m^2
1	2	3	4	5	6	7	8	9	10	11	12

Figure 15: Reduced E values in bottom most cells

These reduced E values were only applied in the horizontal direction while keeping the vertical E value as 15kN/mm^2. After applying a temperature drop of -30ºC, results are as shown in Figure 16a to Figure 16d.

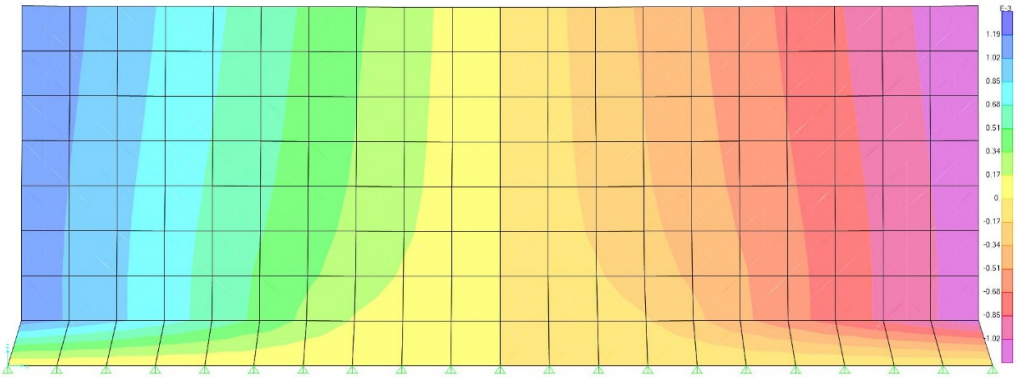

Figure 16a: Deflected shape – technique 1

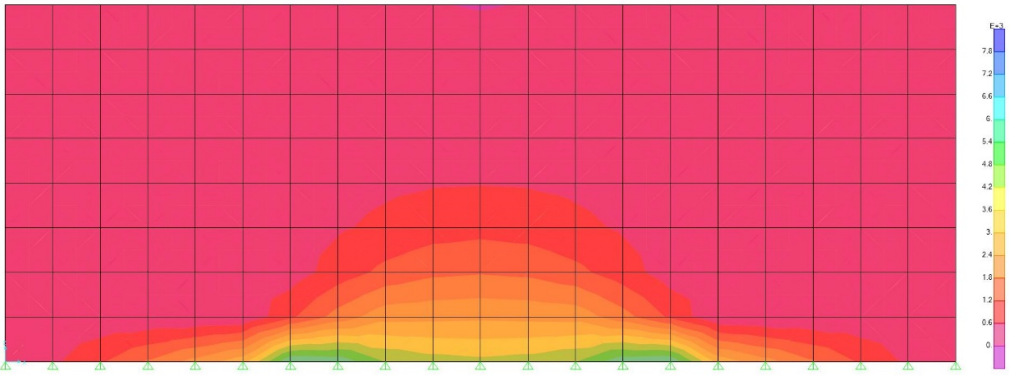

Figure 16b: Maximum stress contour – technique 1

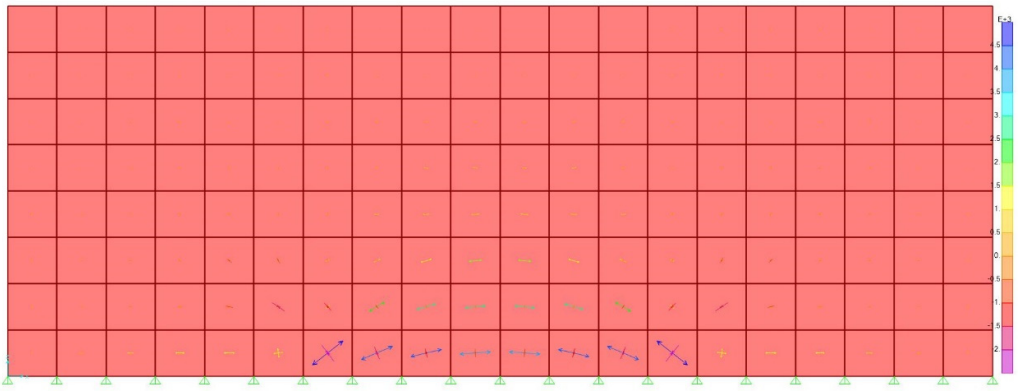

Figure 16c: Principal stresses – technique 1

Fx (kN)	-3.06	33.9	91.12	152.92	215.07	285.58	-251.66	-362.13	-192.34	-86.58	0
Fy (kN)	-17.05	-30.23	-25.93	-24.88	-25.09	-51.10	-308.55	126.83	141.50	144.01	141.01
Node	1	2	3	4	5	6	7	8	9	10	11

Figure 16d: Reactions (left half) – technique 1

3.1.2 Technique 2 – End Rollers with Applied Forces

Possibility of representing the partial restraints at the end 2.4m were considered with rollers. Providing a set of rollers allow the entire 2.4m at the edge to contract freely. However, the restraints should start from zero at the edge and should become full at the end of 2.4m.

In order to provide the partial restraint, an opposing force was applied to each node using the following method;

Step 1 – Model was run with end rollers without any force applied
Step 2 – Sum of the forces in half the wall (4m section) was taken
Step 3 – Node numbers were given for the rollers from n=1 to n=6
Step 4 – Total force per half wall then distributed along the nodes as per Equation 1

$$F_n = \frac{(n-1)}{\sum n} \times \sum F \times \frac{2.4}{(L/2)} \qquad \text{Equation (1)}$$

Where;
n = Node number
F_n = Force at node
$\sum F$ = Total force over a half a length of the wall
L = Total length of the wall

For the 8m wall used, with the initial model with no forces it was found that;
$\sum F = 1249kN$

Force application on each node is shown in Table 02.

Table 02: Nodal Forces

n	F_n (kN)
1	0
2	35.69
3	71.37
4	107.06
5	142.74
6	178.43

With a temperature drop of -30ºC, the results are shown in Figure 17a to Figure 17d.

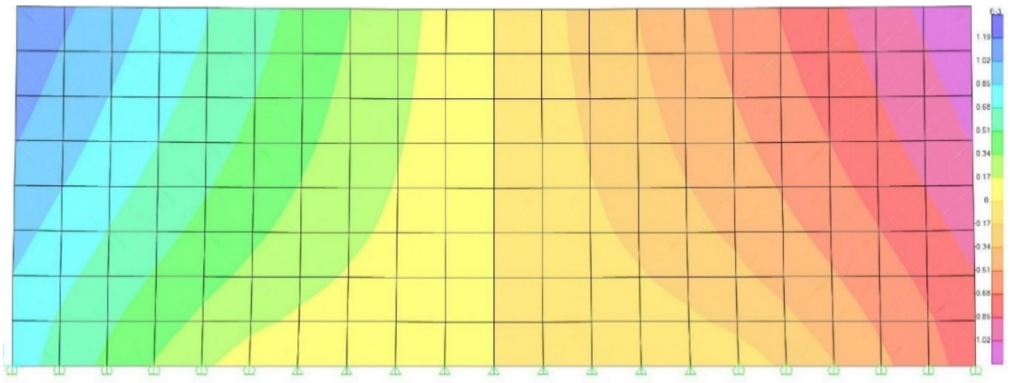

Figure 17a: Deflected shape – technique 2

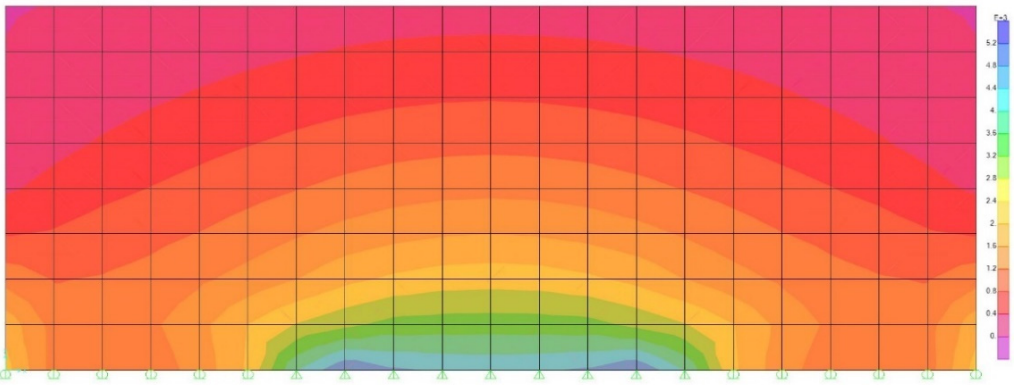

Figure 17b: Maximum stress contour – technique 2

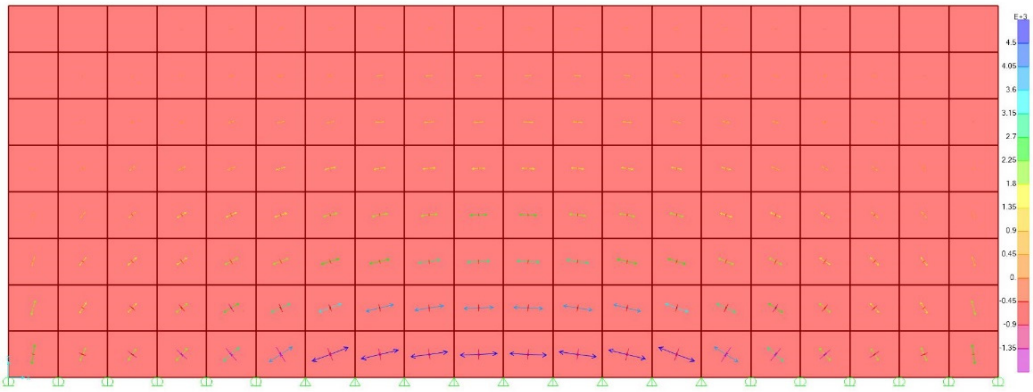

Figure 17c: Principal stresses – technique 2

Fx (kN)	0*	-35.69*	-71.37*	-107.06*	-142.74*	-178.43*	-360.52	-186.96	-108.15	-50.8	0
Fy (kN)	-148.71	-202.71	-122.18	-75.58	-35.18	8.87	81.54	134.62	141.38	145.02	145.87
Node	1	2	3	4	5	6	7	8	9	10	11

Figure 17d: Reactions (left half) – technique 2
(* - applied forces)

3.1.3 Selecting the Best Method and Refinement

In order to choose the best method out of two techniques used, four parameters were considered and the summary is as shown in Table 03.

Table 03: Comparison of two Techniques

	Technique 1	**Technique 2**
Deflected Shape	Deflected shape does not match with the expected shape	Deflected shape matches with the expected shape
Principal stress direction	As expected thus giving expected possible crack pattern	As expected thus giving expected possible crack pattern
Reactions	Irregular variation	Smooth variation

From these results, it is evident that the crack pattern, deflected shape and curling effect is accurately represented by Technique 2. Therefore, it was decided to proceed with Technique 2 as the best method.

As the next step, the mesh was refined to a 0.2m x 0.2m. The process of force distribution was then carried out as shown in Table 04.

With the refined mesh, with the initial model with no forces it was found that;
$\sum F = 1217.91kN$

If we denote the total of initial forces distributed to the nodes by $\sum F_i$;

$$\sum F_i = \sum F \times \frac{2.4}{(L/2)} = 1217.9 \times \frac{2.4}{(8/2)}$$
$$\sum F_i = 730.74kN$$

Table 04: Nodal Forces - 8m wall with base restraints – 1st Iteration

n	F_n (kN)
12	121.79
11	110.72
10	99.65
9	88.58
8	77.50
7	66.43
6	55.36
5	44.29
4	33.22
3	22.14
2	11.07
1	0.00

Then if we denote the resultant forces in the pin joints upto the middle by $\sum F_j$, $\sum F$ should be equal to $\sum F_i + \sum F_j$. From the model results, $\sum F_j = 772.40kN$.

$\therefore \sum F = \sum F_i + \sum F_j = 730.74 + 772.40 = 1503.15kN$

However, it was noticed that there is a difference between the total forces before and after nodal force application. Therefore, it was decided to run another iteration with the new total force to get the forces as close to each other as possible.

For iteration 2;

$\sum F = 1503.151kN$

$$\sum F_i = \sum F \times \frac{2.4}{(L/2)} = 1503.15 \times \frac{2.4}{(8/2)}$$
$$\sum F_i = 901.89kN$$

Corresponding nodal forces for the second iteration are tabulated in Table 05.

Table 05: Nodal Forces - 8m wall with base restraints – 2nd Iteration

n	F_n (kN)
12	150.31
11	136.65
10	122.98
9	109.32
8	95.65
7	81.99
6	68.32
5	54.66
4	40.99
3	27.33
2	13.66
1	0.00

From the model results, $\sum F_j = 667.97$kN.

$\therefore \sum F = \sum F_i + \sum F_j = 901.89 + 667.97 = 1569.86\text{kN} \approx 1503.151\text{kN}$

Therefore, we can use the model results after the second iteration. The results are shown in Figure 18a to Figure 18d.

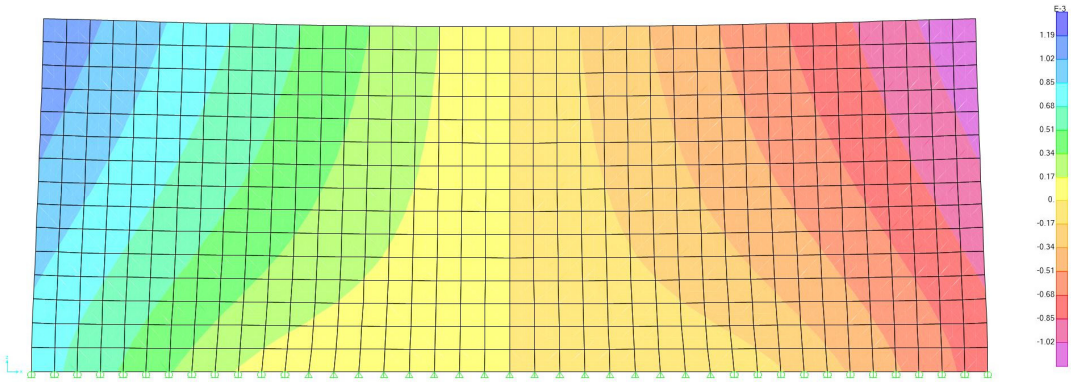

Figure 18a: Deflected shape – 8m wall with base restraint

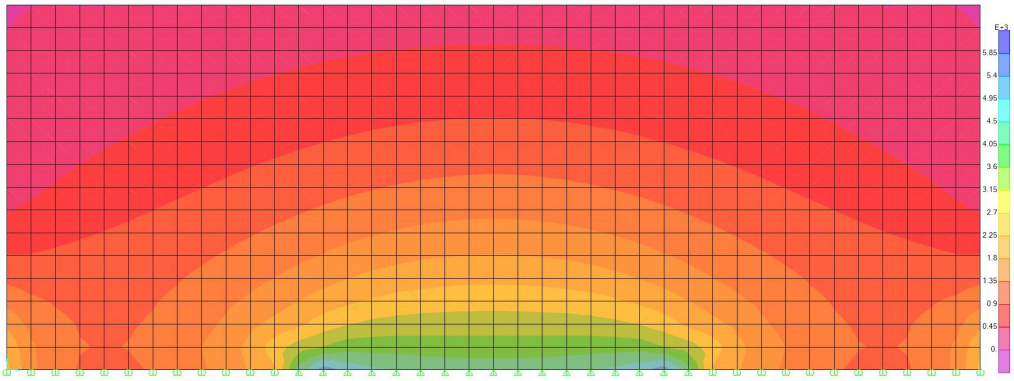

Figure 18b: Maximum stress contour – 8m wall with base restraint

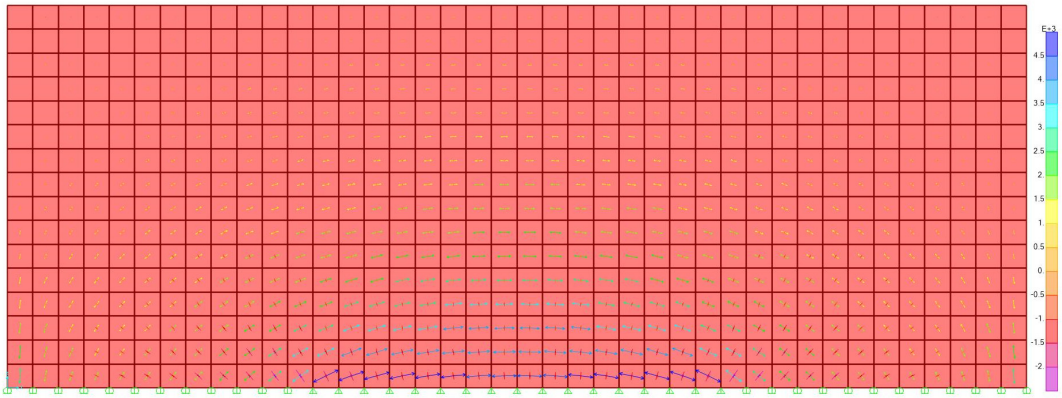

Figure 18c: Principal stresses – 8m wall with base restraint

Fx (kN)	0*	-13.66*	-27.33*	-40.99*	-54.66*	-68.32*	-81.99*	-95.65*	-109.32*	-122.98*	-136.65*
Fy (kN)	-80.50	-125.68	-92.36	-72.33	-57.88	-46.41	-36.47	-27.39	-18.42	-9.58	-0.25
Node	1	2	3	4	5	6	7	8	9	10	11
Fx (kN)	-150.31*	-224.82	-134.43	-98.19	-74.70	-56.17	-40.48	-26.25	-12.94	0	
Fy (kN)	6.43	36.00	65.12	67.55	69.27	70.41	71.48	72.11	72.57	72.6	
Node	12	13	14	15	16	17	18	19	20	21	

Figure 18d: Reactions (left half) – 8m wall with base restraint
(* - applied forces)

3.2 Determining the Variation of End Roller Forces for Walls with L≤4.8m

The process in section 3.1.3 work only when the total wall length is greater than 4.8m. In order to get the end roller forces for walls less than 4.8m in length, walls of 6m, 8m, 10m, 12m up to 22m in length were analysed and the end roller forces were tabulated. (Refer Table 06)

Table 06: Variation of end roller forces

Wall Length (m)	End Roller Forces (kN)	Total Force (kN)	Force/m (kN/m)
6	736.67	1896.50	316.08
8	901.90	3139.60	392.45
10	1011.55	4279.26	427.93
12	1038.91	5230.32	435.86
14	1021.32	5975.12	426.79
16	982.91	6560.82	410.05
18	932.27	6988.16	388.23
20	875.88	7300.66	365.03
22	813.16	7526.36	342.11

The results are shown in the graphs shown in Figure 19a and Figure 19b.

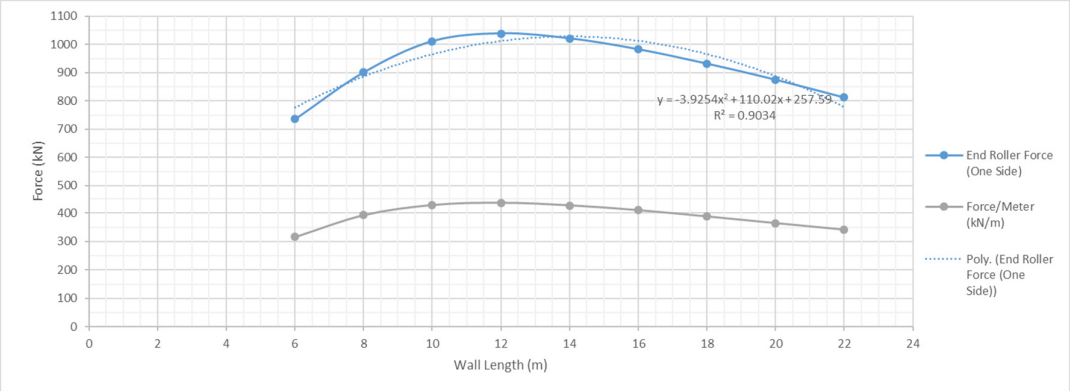

Figure 19a: End roller forces/ Force per meter vs wall length

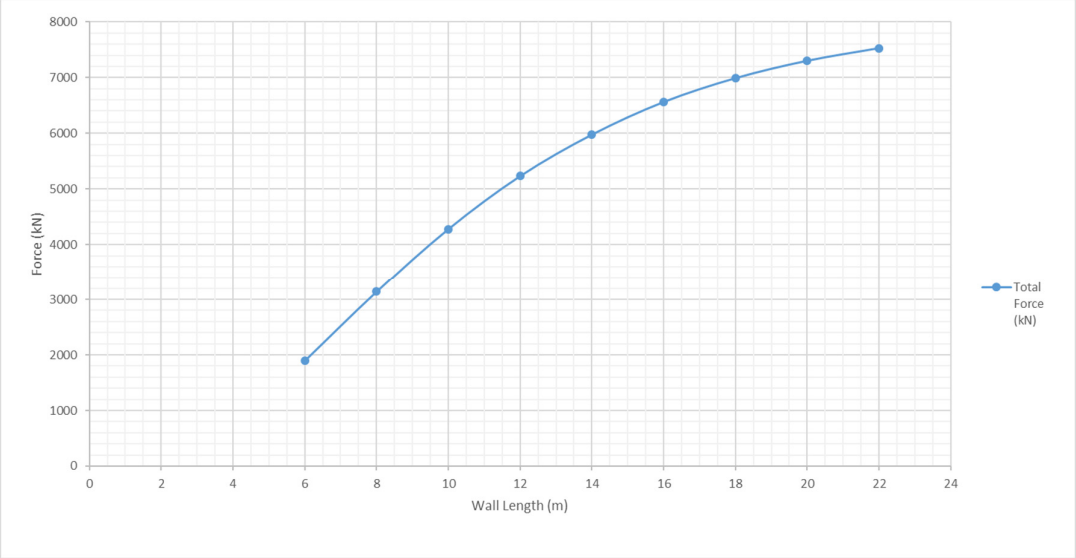

Figure 19b: Total force vs wall length

A polynomial curve was fit to the end roller force variation and using that, the corresponding end roller forces for walls of length less than 4.8m was obtained. (Refer Table 07)

Table 07: Predicted end roller forces for walls <4.8m

Length (m)	**End Roller Force (kN)**
1	363.68
2	461.93
3	552.32
4	634.86

3.3 Imposition of Overall Lateral Displacement Along Top Edge due to Temperature Movement

As discussed in section 2.2, movements due to temperature of the overall slab can induce a movement on the shear walls on top which will create dominant cracks as shown in Figure 13. Since the edge walls are more susceptible to this movement, 8m long, 3m high, 300mm thick wall at a building edge was considered. Length of the building in plane of the wall is taken as 40m. Considering the temperature movement will be zero at the centre and maximum at the edge, temperature movement for half a building length is calculated for a 30ºC temperature drop as follows;

$\Delta = L\alpha\theta$ Equation (2)

Where;

Δ = Temperature movement

L = Length of the element

α = Coefficient of thermal expansion

θ = Temperature difference

$\Delta = L\alpha\theta = 20000 \times 10^{-5} \times 30$

$= 6mm$

Since the movement is maximum at the edge and it is reducing to zero at the centre of the building, assuming a linear variation a movement varying from 6mm to 3.6mm along the wall is applied. The resulting principal stress diagram is shown in Figure 20.

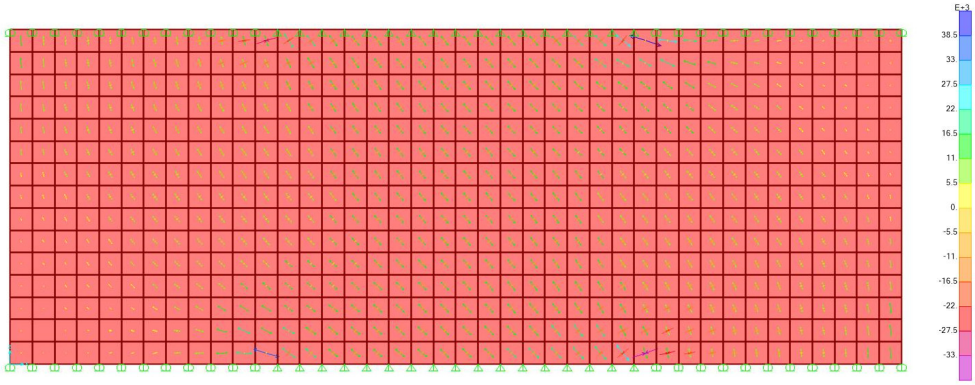

Figure 20: Principal Stresses – 8m wall with top and bottom restraints – top movement

Comparing the principal stress directions and thus the possible crack pattern shows a complete opposite to the actual scenario shown in Figure 13. It is believed that the difference is due to the fact that actual movement will be considerably lesser than the calculated 6mm as free contraction of the slab is not possible. Therefore, the model was re-run with a maximum movement of 0.6mm reducing up to 0.36mm at the

opposite end. The results of that are shown in Figure 21a to Figure 21c. This reduction is somewhat arbitrary and has to be studied in future research.

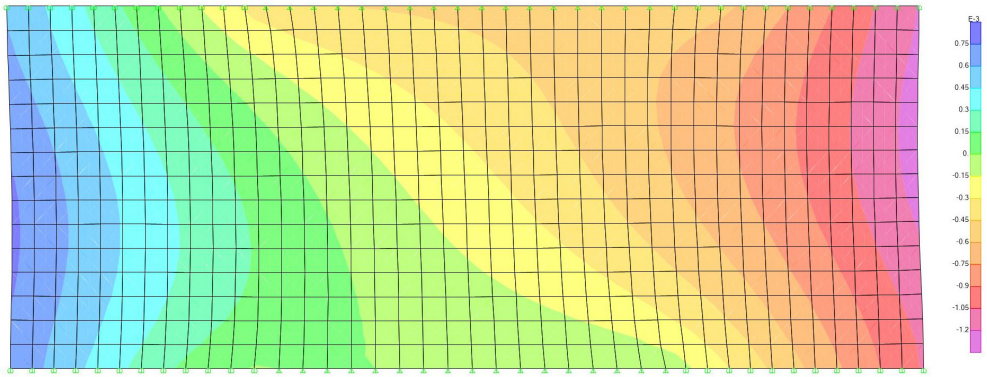

Figure 21a: Deflected Shape - 8m wall with top and bottom restraints – reduced top movement

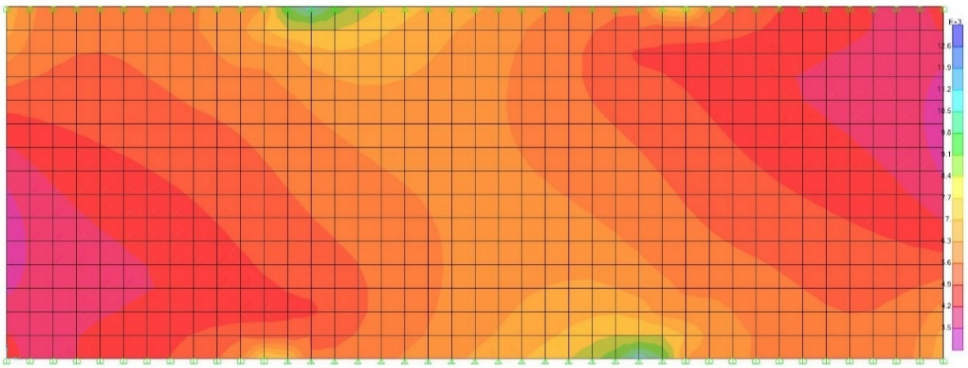

Figure 21b: Maximum Stress Contour - 8m wall with top and bottom restraints – reduced top movement

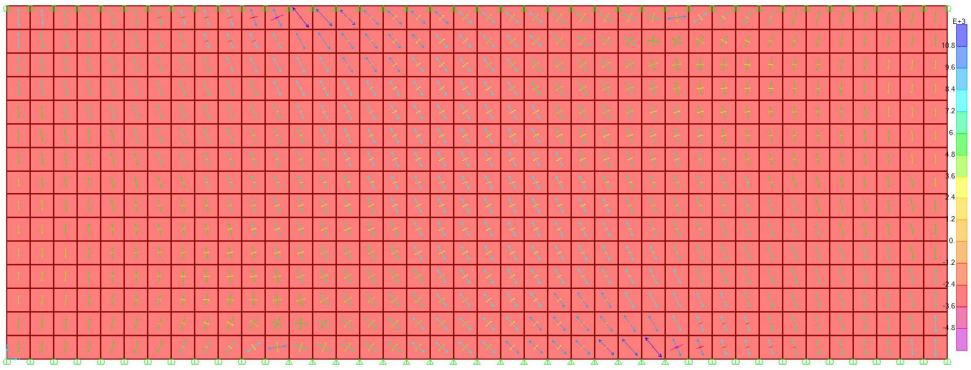

Figure 21c: Principal Stresses - 8m wall with top and bottom restraints – reduced top movement

With the reduced movement, principle stress pattern and thus the possible crack pattern matches with the crack pattern observed in section 2.2.

4 Results of Case Studies

Six different case studies for two different wall sizes were carried out using the methods described in the section 3 and compared with crack patterns provided in BS8007 and other literature. All the walls considered were 3m in height and 300mm in thickness. Two lengths of 8m and 4m were used for the case studies. The following conditions were modelled;

1. Base restraint
2. Top and bottom restraint
3. Top and bottom restraint with movement at top

4.1 8m Wall with Base Restraint

Wall is restrained only in the base and roller supports are provided for a length of 2.4m from either end. Middle nodes are pinned. Applied Nodal forces are as per Table 08 after the second iteration.

Table 08: Nodal Forces - 8m wall with base restraints – 2nd Iteration

n	F_n (kN)
12	150.31
11	136.65
10	122.98
9	109.32
8	95.65
7	81.99
6	68.32
5	54.66
4	40.99
3	27.33
2	13.66
1	0.00

Model results are shown in Figure 22a to 22c.

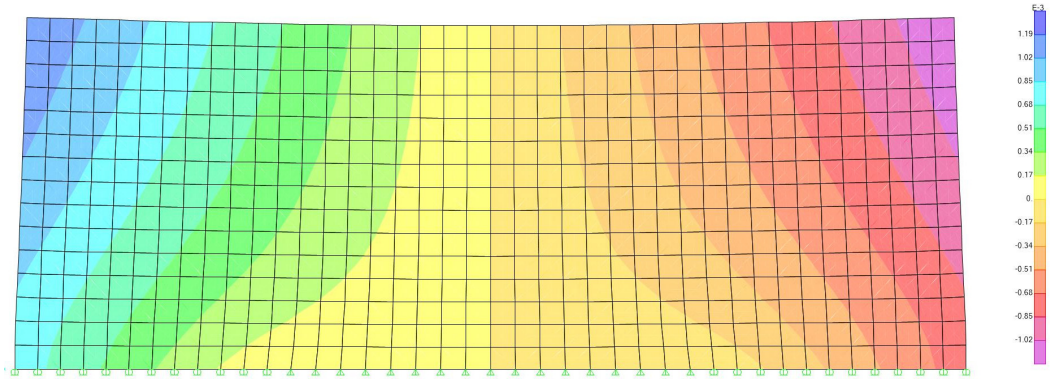

Figure 22a: Deflected Shape - 8m wall with bottom restraint

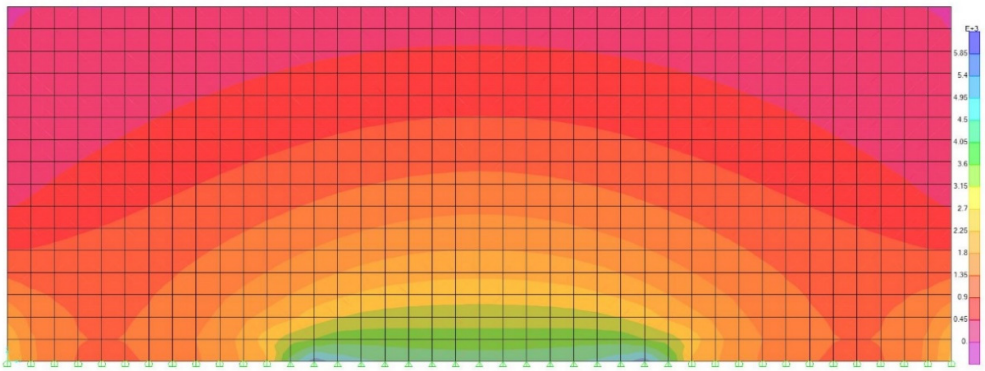

Figure 22b: Maximum Stress Contour - 8m wall with bottom restraint

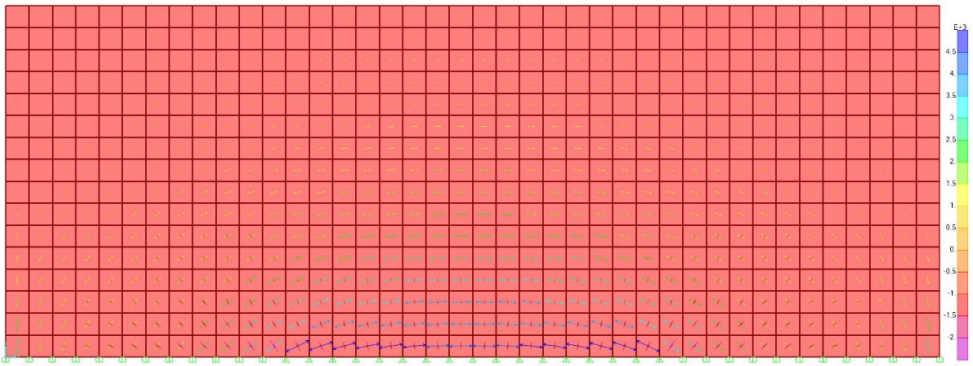

Figure 22c: Principal Stresses - 8m wall with bottom restraint

It is observed that most probable locations where cracks would occur are at 2.4m from either end and they would be diagonal (Refer Figure 22d) according to the principal stress pattern as expected. It should however be noted that this is not to indicate that the given stress produces cracking but to that the stress is maximum at the given direction & location and that it is the most likely combination for a crack to form. (All such diagrams henceforth follow the same assumption)

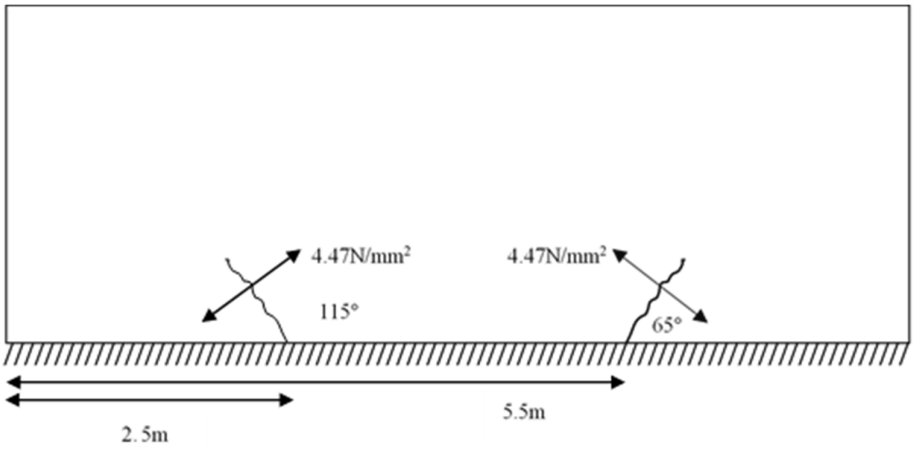

Figure 22d: Observed possible crack pattern - 8m wall with bottom restraint

4.2 8m Wall with Top and Bottom Restraint

Wall is restrained along top and bottom faces. Roller supports are provided for a length of 2.4m from either end for both top and bottom faces. Middle nodes are pinned. Applied Nodal forces on the bottom face are as per Table 09 and on the top face are as per Table 10 after the second iteration.

Vertical movement of the nodes at top are restricted considering the restraint which will be provided by the slab/beams cast together and the formwork system.

Table 09: Nodal Forces Bottom - 8m wall with top and bottom restraints – 2nd Iteration

n	F_n (kN)
12	146.71
11	133.37
10	120.03
9	106.70
8	93.36
7	80.02
6	66.68
5	53.35
4	40.01
3	26.67
2	13.34
1	0.00

Table 10: Nodal Forces Top - 8m wall with top and bottom restraints – 2nd Iteration

n	F_n (kN)
12	146.71
11	133.37
10	120.03
9	106.70
8	93.36
7	80.02
6	66.68
5	53.35
4	40.01
3	26.67
2	13.34
1	0.00

Model results are shown in Figure 23a to 23c.

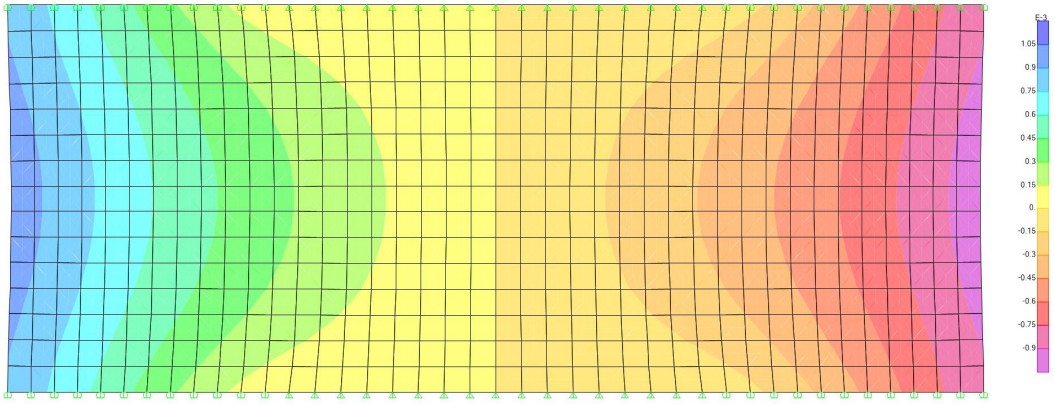

Figure 23a: Deflected Shape - 8m wall with top and bottom restraints

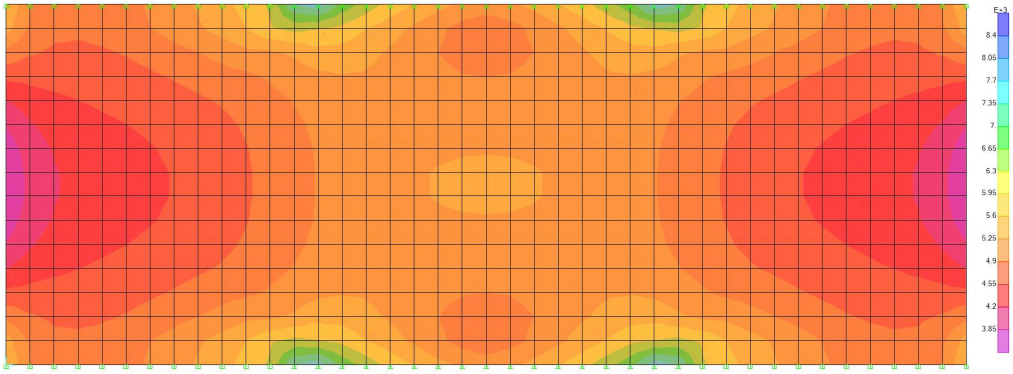

Figure 23b: Maximum Stress Contour - 8m wall with top and bottom restraints

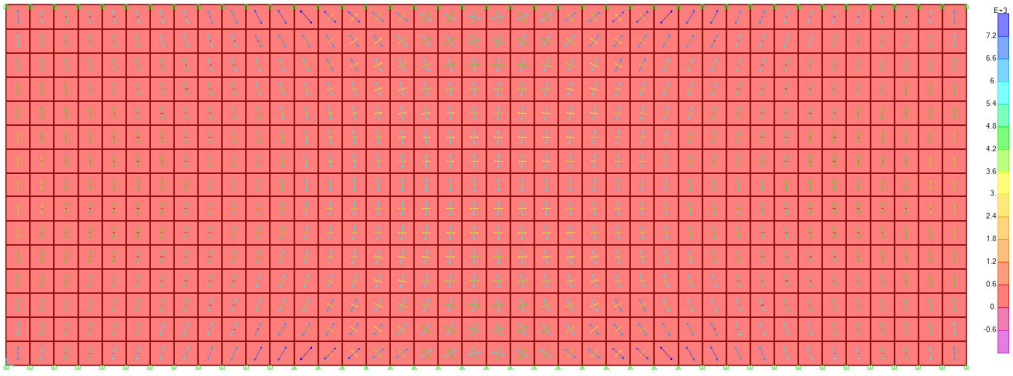

Figure 23c: Principal Stresses - 8m wall with top and bottom restraints

Four dominant possible cracks were observed according to the maximum principal tensile stresses. These were located top and bottom on either side 2.4m away from the edges. Angle of the cracks were 45º and 135º approximately. (Refer Figure 23d)

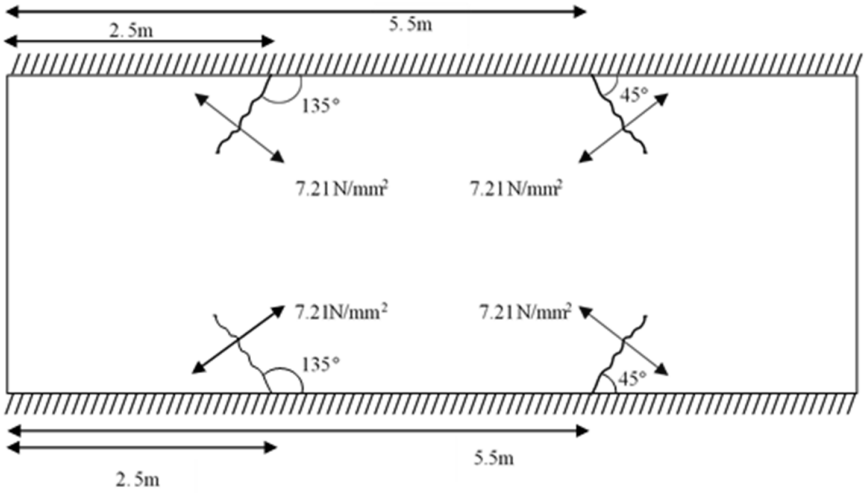

Figure 23d: Observed possible crack pattern - 8m wall with top and bottom restraints

4.3 8m Wall with Top and Bottom Restraint with Movement at Top

Wall is restrained along top and bottom faces. Roller supports are provided for a length of 2.4m from either end for both top and bottom faces. Middle nodes are pinned. Applied Nodal forces on the bottom face are as per Table 09 and on the top face are as per Table 10 after the second iteration.

Vertical movement of the nodes at top are restricted considering the restraint which will be provided by the slab/beams cast together and the formwork system.

A horizontal movement varying from 0.6mm to 0.36mm is applied to the top face as discussed in section 3.3 to simulate the thermal movement from the slab.

Model results are shown in Figure 24a to 24c.

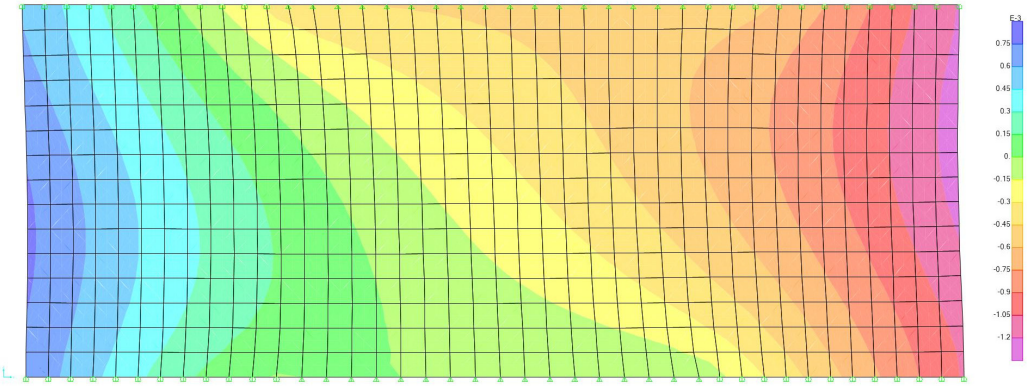

Figure 24a: Deflected Shape - 8m wall with top and bottom restraints – top movement

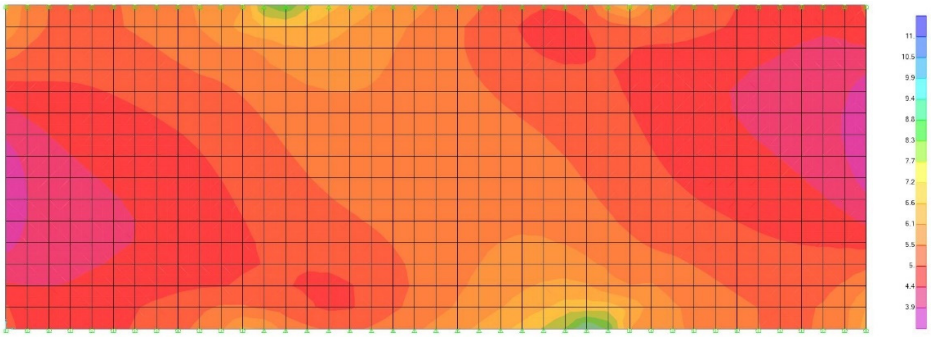

Figure 24b: Maximum Stress Contour - 8m wall with top and bottom restraints – top movement

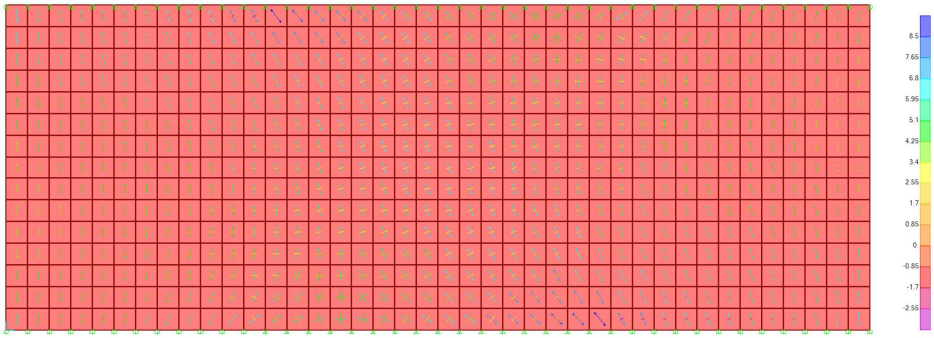

Figure 24c: Principal Stresses - 8m wall with top and bottom restraints – top movement

According to the principal stresses, two dominant possible cracks, one at 2.4m from the left on top and the other at 2.4m from the right at the bottom were observed. Top crack observed at an angle of 105º while the bottom crack was observed at an angle of 75º (Refer Figure 24d). This observation conforms to the crack pattern observed according to section 2.2.

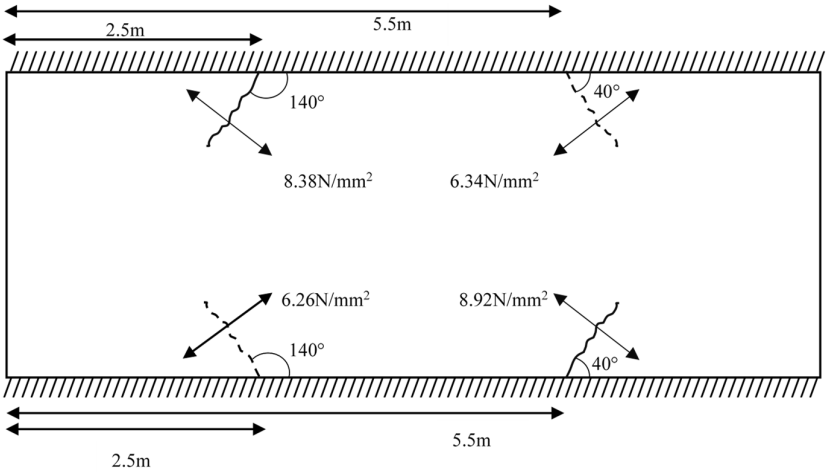

Figure 24d: Observed possible crack pattern - 8m wall with top and bottom restraints – top movement

4.4 4m Wall with Base Restraint

Wall is restrained only in the base and roller supports are provided for all the nodes except for the middle node. Middle node is pinned to ensure the stability. As the lateral force on the middle node is zero, this does not affect the results. Applied Nodal forces are as per Table 11 according to section 3.2.

Table 11: Nodal Forces - 4m wall with base restraint

n	F_n (kN)
10	126.97
9	112.86
8	98.76
7	84.65
6	70.54
5	56.43
4	42.32
3	28.22
2	14.11
1	0.00

Model results are shown in Figure 25a to 25c.

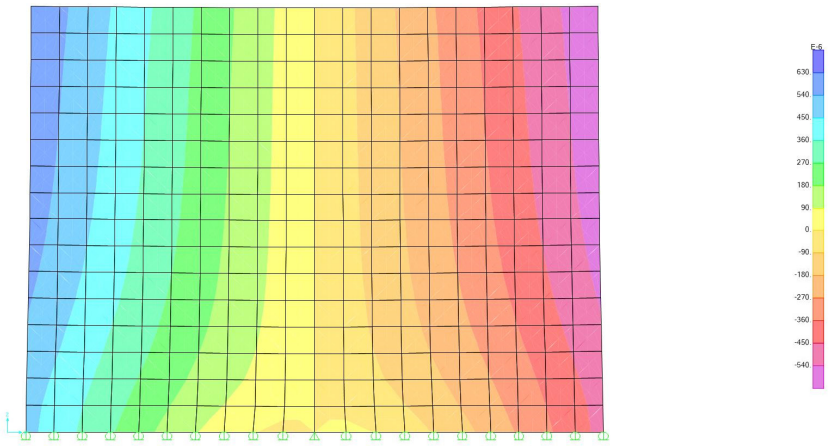

Figure 25a: Deflected Shape - 4m wall with bottom restraint

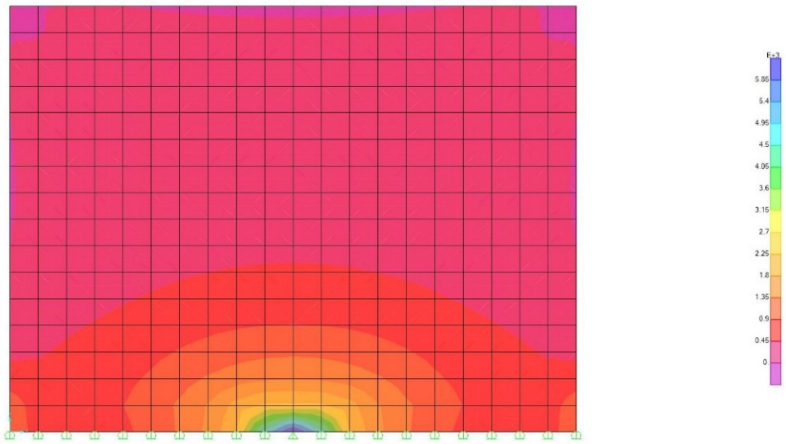

Figure 25b: Maximum Stress Contour - 4m wall with bottom restraint

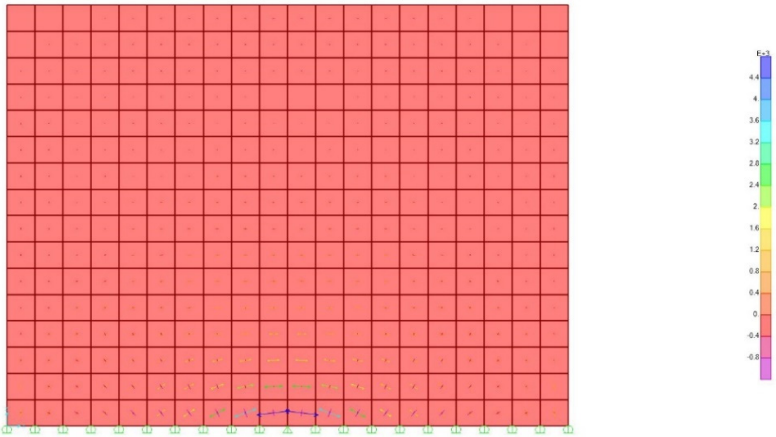

Figure 25c: Principal Stresses - 4m wall with bottom restraint

A possible vertical crack location at the centre was observed according to the principal stress pattern as expected. (Refer Figure 25d)

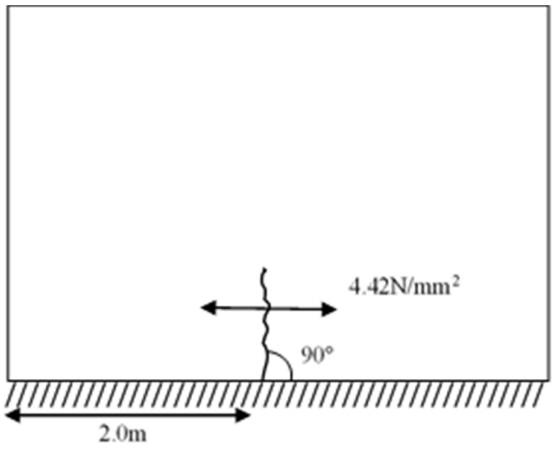

Figure 25d: Observed possible crack pattern - 4m wall with bottom restraint

4.5 4m Wall with Top and Bottom Restraint

Wall is restrained in top and bottom and roller supports are provided for all the nodes except for the middle node. Middle node is pinned to ensure the stability. As the lateral force on the middle node is zero, this does not affect the results. Applied Nodal forces for both the top and bottom are as per Table 11 according to section 3.2.

Vertical movement of the nodes at top are restricted considering the restraint which will be provided by the slab/beams cast together and the formwork system.

Model results are shown in Figure 26a to 26c.

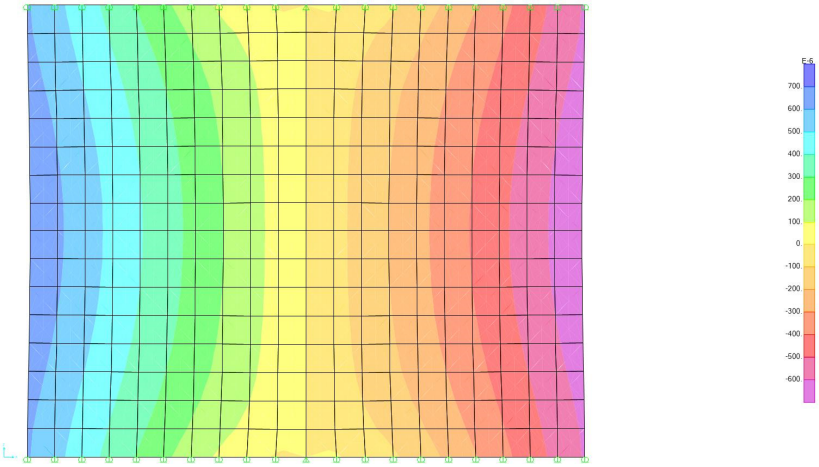

Figure 26a: Deflected Shape - 4m wall with top and bottom restraints

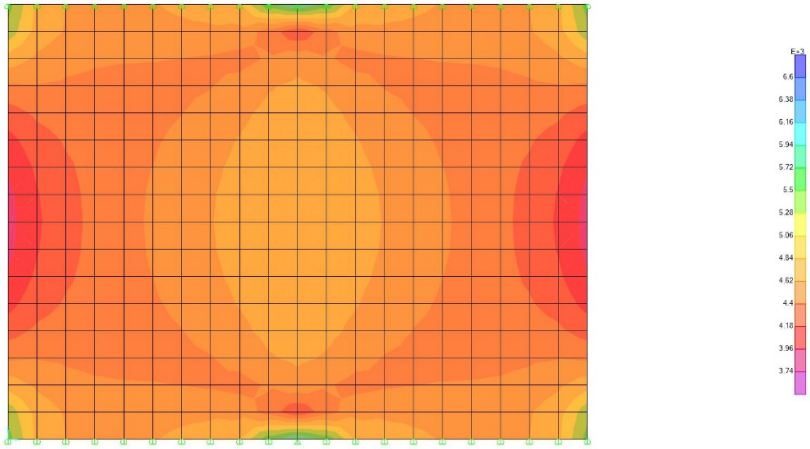

Figure 26b: Maximum Stress Contour - 4m wall with top and bottom restraints

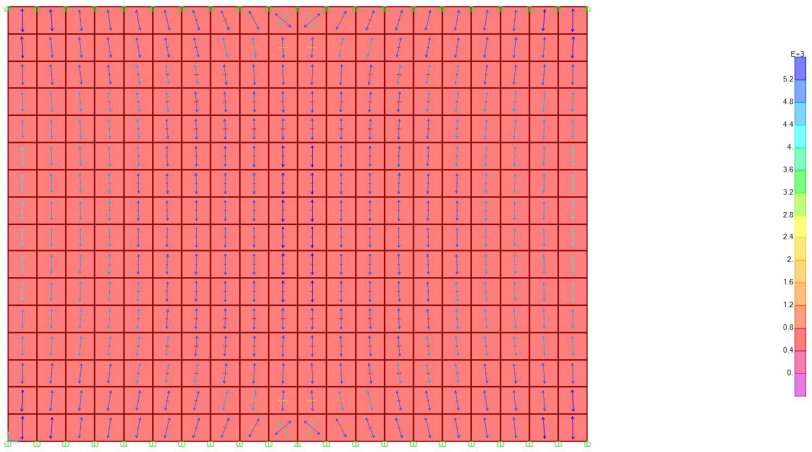

Figure 26c: Principal Stresses - 4m wall with top and bottom restraints

A possible horizontal crack at the centre and vertical cracks 2m away from the free edge are observed according to the principal stress pattern as expected. (Refer Figure 26d)

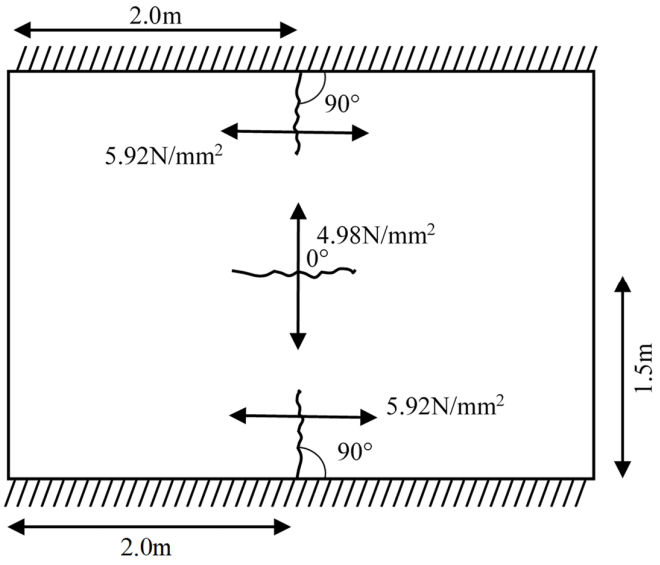

Figure 26d: Observed possible crack pattern - 4m wall with top and bottom restraints

4.6 4m Wall with Top and Bottom Restraint with Movement at Top

Wall is restrained in top and bottom and roller supports are provided for all the nodes except for the middle node. Middle node is pinned to ensure the stability. As the lateral force on the middle node is zero, this does not affect the results. Applied Nodal forces for both the top and bottom are as per Table 11 according to section 3.2.

Vertical movement of the nodes at top are restricted considering the restraint which will be provided by the slab/beams cast together and the formwork system.

A horizontal movement varying from 0.6mm to 0.48mm is applied to the top face as discussed in section 3.3 to simulate the thermal movement from the slab.

Model results are shown in Figure 27a to 27c.

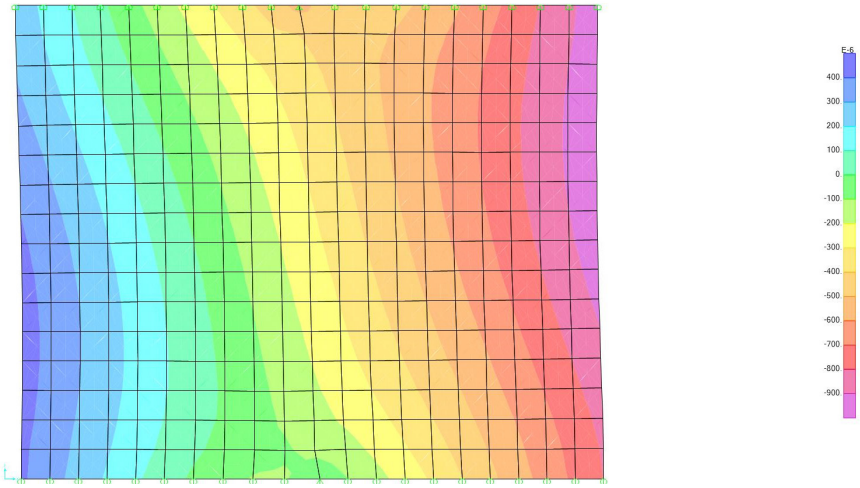

Figure 27a: Deflected Shape - 4m wall with top and bottom restraints – top movement

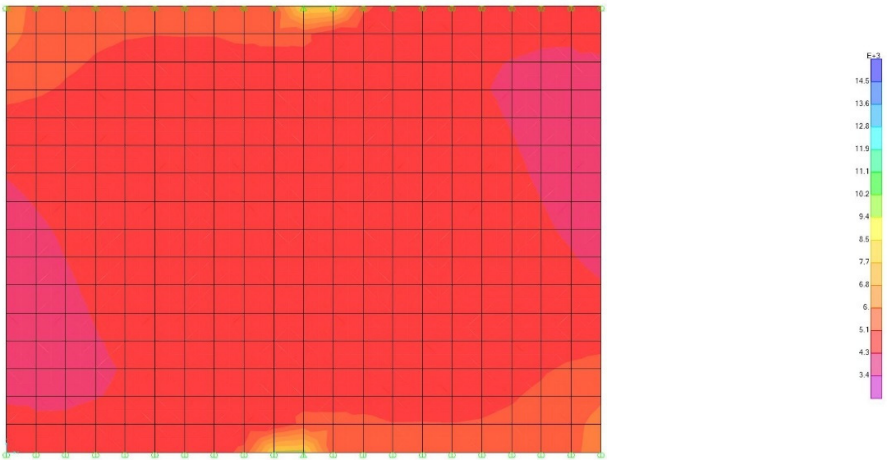

Figure 27b: Maximum Stress Contour - 4m wall with top and bottom restraints – top movement

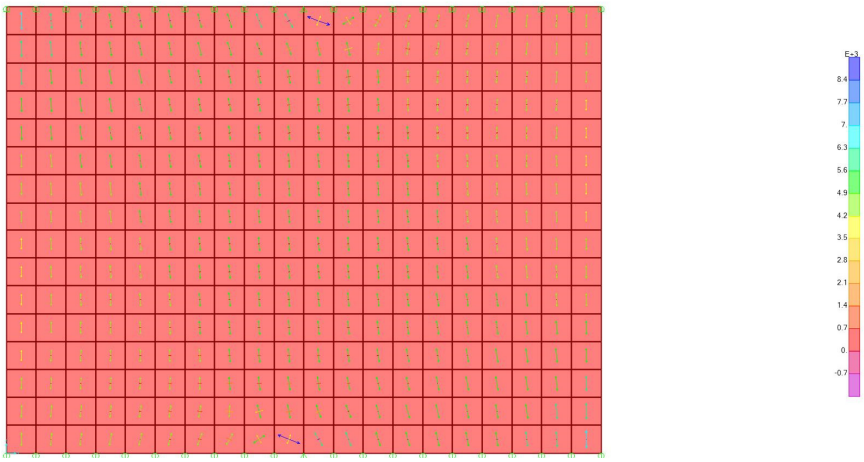

Figure 27c: Principal Stresses - 4m wall with top and bottom restraints – top movement

It is observed that two dominant possible cracks will occur close to the centre on top and bottom at an angle according to the principal stress pattern. (Refer Figure 27d)

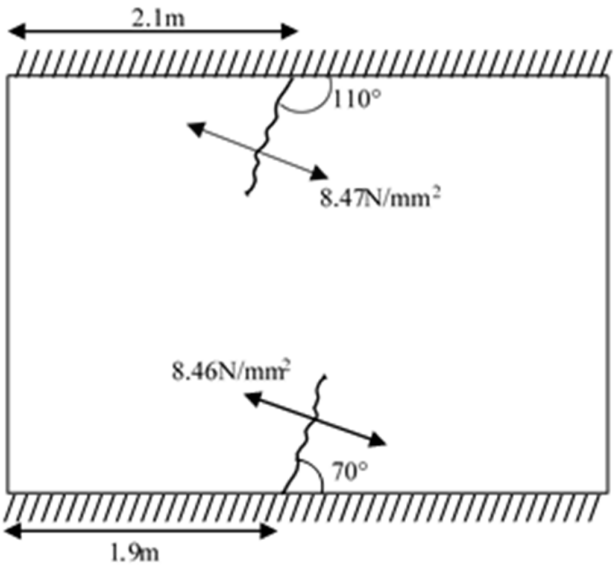

Figure 27d: Observed possible crack pattern - 4m wall with top and bottom restraints – top movement

4.7 Summary and Discussion of Results

Summary of case study results are shown in Table 12.

Table 12: Summary of case study results

Wall Length (m)	Boundary Condition	Distance to the Crack from the near Edge (m)	Location of the Crack	Angle of the Crack (°)	Maximum Principal Stress (N/mm^2)
4	Bottom Restrained	2.00	Bottom	90	4.42
4	Top and Bottom Restrained	1.50	Center	0	4.98
		2.00	Bottom	90	5.92
		2.00	Center	90	5.92
4	Top and Bottom Restrained with Top Movement	1.90 (2.10)	Bottom (Top)	70 (110)	8.46 (8.47)
8	Bottom Restrained	2.50 (5.50)	Bottom (Bottom)	115 (65)	4.47 (4.47)
8	Top and Bottom Restrained	2.50 (5.50)	Bottom (Bottom)	135 (45)	7.21 (7.21)
		2.50 (5.50)	Top (Top)	135 (45)	7.21 (7.21)
8	Top and Bottom Restrained with Top Movement	2.50 (5.50)	Bottom (Bottom)	140 (40)	6.26 (8.92)
		2.50 (5.50)	Top (Top)	140 (40)	8.38 (6.34)

The following general observations can be made;

(i) 8m walls get the highest stress close to 2.4m from the free edges whereas the 4m walls get the highest stress at the centre.

(ii) In 8m walls higher stresses are distributed over a length whereas in 4m walls the higher stress is concentrated at the centre.

(iii) Higher stresses are observed with top movement.

(iv) 4m wall has possible vertical and horizontal cracking (centrally). In the presence of top movement, there are two possible cracks at top and bottom slightly inclined to the vertical at the centre.

(v) 8m wall has possible inclined cracking 2.4m from free edges. In the presence of top movement, possible two dominant crack and 2 minor crack locations can be observed.

5 Conclusions & Recommendations

This research focused on developing a simplified modelling technique to represent early age thermal cracking in concrete walls. Two techniques, reduced E-value technique and end roller forces, were performed to find out the most appropriate method to reduced restraint behaviour. It could be observed that the reduced restraint behaviour is better modelled with end roller force method than the reduced E-value method.

The simultaneous concreting of slab and underlying walls that is increasingly adopted in practice can cause significant top movements in walls that are at building edges and perpendicular to those edges. This condition was modelled with application of lateral movement to the top nodes of the top and bottom restrained walls. In addition, various types of wall behaviours were modelled for both long (>4.8m) and short (<4.8m) walls.

The case studies yielded the following general findings that agree with the literature and field observations with respect to generating maximum stress values and directions that corresponded to observed cracking;

(i) 4m walls can have possible vertical and horizontal cracks.
(ii) 8m walls can have possible cracks approximately 2.4m away from the free edges with an inclination of approximately 45º-60º.
(iii) 8m walls get the highest stress close to 2.4m from the free edges whereas the 4m walls get the highest stress at the centre.
(iv) In 8m walls higher stresses are distributed over a central length whereas in 4m walls the higher stress is concentrated at the centre.
(v) 4m wall with top movement can cause possible inclined cracks.
(vi) 8m wall with top movement can lead to possible two dominant cracks and two minor cracks.

For future research work, checking the validity of the modelling technique for more scenarios and improving the modelling to represent more fundamental mechanisms of creep and bond are suggested.

BS8007 recommends minimum reinforcement to ensure distribution of cracking (Clause A.2, BS8007:1987). This normally concentrates on horizontal reinforcement which distributes the vertical cracks. However, it is evident from our results that for construction methods involving slab and wall concreting simultaneously, there is significant vertical restraint generated in addition to the horizontal restraint throughout the wall. Therefore, the use of minimum reinforcement to distribute cracking is important for vertical reinforcement as well.

References

[1] Klemczak B., Knoppik A.; Early age thermal and shrinkage cracks in concrete structures - Description of the problem, 2011.

[2] Leonhardt F., Cracks and crack control in concrete structures. PCI Journal, July-August 1988.

[3] de Schutter G. and Taerwe L.; General hydration model for Portland cement and blast furnace slag cement. Cement and Concrete Research, 25(3):593–604, 1995.

[4] Schindler A. K.; Concrete hydration, temperature development, and setting at early ages. PhD thesis, University of Texas at Austin, Austin, USA, 2002.

[5] Knoppik A.; Analysis of early-age thermal–shrinkage stresses in reinforced concrete walls. PhD thesis, Silesian University of Technology, Gliwice, Poland, 2015.

[6] Neville A. M. Properties of concrete. Prentice Hall, San Francisco, USA, 5th edition, 2012.

[7] http://www.concrete.org.uk.

[8] Flaga K., Furtak K.; Problem of thermal and shrinkage cracking in tanks, vertical walls and retaining walls near their contact with solid foundation slabs. Architecture-Civil Engineering-Environment, Vol.2, No.2/2009, p.23-30.

[9] BS8007 - Code of practise for Design of concrete structures for aqueous liquids. BSI, UK, 1987.